

Dynamic analysis of a simply supported beam resting on a nonlinear elastic foundation under compressive axial load using nonlinear normal modes techniques under three-to-one internal resonance condition

Ahmad Mamandi · Mohammad H. Kargarnovin · Salman Farsi

Received: 1 May 2011 / Accepted: 22 June 2012 / Published online: 21 July 2012
© The Author(s) 2012. This article is published with open access at Springerlink.com

Abstract In this paper, the *Nonlinear Normal Modes (NNMs)* analysis for the case of three-to-one (3:1) internal resonance of a slender simply supported beam in presence of compressive axial load resting on a nonlinear elastic foundation is studied. Using the Euler–Bernoulli beam model, the governing nonlinear PDE of the beam’s transverse vibration and also its associated boundary conditions are extracted. These nonlinear motion equation and boundary condition relations are solved simultaneously using four different approximate-analytical solution techniques, namely *the method of Multiple Time Scales, the method of Normal Forms, the method of Shaw and Pierre, and the method of King and Vakakis*. The obtained results at this stage using four different methods which are all in time–space domain are compared and it is concluded that all the methods result in a similar answer for the amplitude part of the transverse vibration. At the next step, the nonlinear normal modes are

obtained. Furthermore, the effect of axial compressive force in the dynamic analysis of such a beam is studied. Finally, under three-to-one-internal resonance condition the NNMs of the beam and the steady-state stability analysis are performed. Then the effect of changing the values of different parameters on the beam’s dynamic response is also considered. Moreover, 3-D plots of stability analysis in the steady-state condition and the beam’s amplitude frequency response curves are presented.

Keywords Beam’s nonlinear dynamics · Nonlinear elastic foundation · The 3:1 internal resonance · Steady-state stability analysis · Beam’s frequency response

1 Introduction

The problem of dynamic analysis of uniform slender beam resting on elastic foundation subjected to axial loading is very common in structural systems under actual operating conditions. Hence, from the past decades the linear and nonlinear analysis of such systems is one of the important topics in many engineering fields, especially civil and railway engineering. More specifically, in the design of structural components in buildings, aircrafts, ships, buried pipes, concrete pavement slabs and bridges etc. One of the most essential types of external forces would be in-plane compressive forces due to either pre-stressing or

A. Mamandi (✉)
Department of Mechanical Engineering, Parand Branch,
Islamic Azad University, Tehran, Iran
e-mail: am_2001h@yahoo.com

M.H. Kargarnovin
Department of Mechanical Engineering, Sharif University
of Technology, Tehran, Iran
e-mail: mhkargar@sharif.edu

S. Farsi
Department of Mechanical Engineering, Tarbiat Modares
University, Tehran, Iran

changes in the environmental conditions such as temperature and moisture. For instance, when surrounding temperature increases, rails, beams, concrete slabs, etc. tend to expand and compressive forces are induced if there are some essential boundary constraints on these elements. Due to these induced in-plane compressive forces, these elements some times may experience buckling phenomenon. The in-plane compressive forces are also present in pre-stressed beams. Moreover, in working conditions these beams are almost resting on a foundation. In practice and from engineering point of view, the most well-known foundations are classified as elastic, viscoelastic, Winkler and Pasternak. In the last decades the combined effects of foundation stiffness and the in-plane compressive forces have attracted the attention of many researchers working in the field of structural analysis.

The cases of three-to-one and one-to-one internal resonances for the nonlinear free vibrations of a fixed-fixed buckled beam about its first post-buckling configuration is studied in Ref. [1]. In this study, the *NNMs* approach is used by implementing Multiple Time Scales method (*MTS*) directly to the governing PDE of motion as well as its BCs. In Ref. [2], nonlinear vibrations and instabilities of an elastic beam resting on a nonlinear elastic foundation are investigated using analytical and semi-analytical perturbation methods. Also, Melnikov's method is applied to determine an algebraic expression for the boundary that separates the safe from the unsafe region in the force parameters space. Dynamics of nonlinear problem of non-uniform beams resting on a nonlinear triparametric elastic linear and nonlinear Winkler and also linear Pasternak foundation is presented in Ref. [3] where the solution is obtained using the analog equation method of Katsikadelis. In Ref. [4], by using the method of perturbation, the governing PDE of static deflection of a general elastically end-restrained non-uniform beam resting on a nonlinear elastic foundation subjected to axial and transverse loads is solved. A new method using the differential quadrature method (*DQM*) is applied in Ref. [5] for the dynamic analysis of non-uniform beams resting on nonlinear foundations. The obtained results solved using the *DQM* have excellent agreement with the results solved using the FEM analysis. In Ref. [6], the integro-differential equations of motion governing nonlinear vibrations of a slightly curved beam with immovable simply supported ends resting on a nonlinear elastic foundation are solved using the method

of *MTS*. The amplitude and phase modulation equations are derived for the case of primary resonances. Both free and forced vibrations with damping are investigated. It is found that the effect of curvature is of softening type and the elastic foundation may suppress the softening behavior resulting in a hardening behavior of the nonlinearity. In Ref. [7], the differential equation describing the nonlinear dynamics of a simply supported beam resting on a nonlinear spring foundation with cubic stiffness is analyzed and then discretized using Galerkin procedure and its nonlinear dynamic behavior is investigated using the method of Normal Forms (*NFs* method). The possibility of the model to exhibit primary, superharmonic, subharmonic and internal resonances has been investigated and the singular perturbation approach is used to study both the free and the forced oscillations of the beam. In Ref. [8], the differential transform method (*DTM*) is employed to predict induced vibration in pipelines resting on an elastic soil bed via the Euler–Bernoulli and Timoshenko beams models. In Ref. [9], the effects of nonlinear elastic foundation on free vibration of beams is investigated. In Ref. [10], energy-based *NNMs* methodologies are applied to a canonical set of equations and asymptotic solutions are obtained for computing the resonant nonlinear normal modes (*NNMs*) for discrete and continuous systems. This work was extended to study the 3:1 resonances in a two-degree-of-freedom system and 3:1 resonance in a hinged-clamped beam. In Ref. [11], a simply-supported beam lying on a nonlinear elastic foundation and a cantilever beam possessing geometric nonlinearities are considered and their partial differential equations are asymptotically solved using a perturbation method by computing the nonlinear normal modes. In Ref. [12], the concept of nonlinear normal mode is used to study localized oscillations for continuous systems of finite and infinite length. Moreover, the implications of nonlinear mode localization on the vibration and shock isolation of periodic flexible structures are discussed. In Ref. [13], an energy-based method is used to obtain the *NNMs* of a slender beam resting on an elastic foundation with cubic nonlinearity under an axial tensile load. Also, a double asymptotic expansion is performed to capture the boundary layer in the nonlinear mode shape due to the small bending stiffness of the beam. In Ref. [14], a numerical method based on invariant manifold approach is presented to construct *NNMs* for sys-

tems with internal resonances. The computationally-intensive solution procedure is used as a combination of finite difference schemes and Galerkin-based expansion approaches. Moreover, two examples are studied. In the first example an invariant manifold that captures two nonlinear normal modes is constructed for a simple three-degree-of-freedom system. The methodology is then applied to an 18-degree-of-freedom rotating beam model that features a three-to-one internal resonance between the first two flapping modes. In Ref. [15], systematic methods are developed for generating minimally sized reduced-order models that describe the vibrations of large-scale nonlinear engineering structures. The general approach in the phase space of the system model uses the *NNMs* that are defined in terms of invariant manifolds. To construct *NNMs* that are accurate to large amplitudes of vibration, the Galerkin projection method is developed. This approach is extended to construct the *NNMs* for systems with internal resonance subjected to external excitation. Furthermore, the Galerkin-based construction of the nonlinear normal modes is also applied for a rotating beam. A derivation of nonlinear equations governing the dynamics of an axially loaded beam is studied in Ref. [16] where two load cases are considered; primarily a structure is subjected to a uniformly distributed axial load and in the other case to a thrust force for modeling an offshore riser. The *NNMs* and nonlinear multi-modes (*NMMs*) have been constructed by using the method of multiple time scales. The dynamic transverse response of the beam has been calculated by monitoring the modal responses and beam's mode interactions. Moreover, the FEM analysis has been performed. The comparisons of the dynamical responses are made in terms of time histories, phase portraits and mode shapes. The evidence of the nonlinear normal modes in the forced response of a non-smooth piecewise two-degree-of-freedom system and bifurcations characterized by the onset of superabundant modes in internal resonance conditions is investigated in Ref. [17]. In Ref. [18], the classical Lindstedt–Poincaré method for evaluating nonlinear normal modes of a piecewise linear two-degree-of-freedom system is adapted to analyze the nonlinear normal modes of a simple piecewise linear two-degree-of-freedom system representing a beam with a breathing crack. In this study, numerical results obtained by a Poincaré map approach show the existence of superabundant normal modes which arise in the unstable interval of the first mode and can be predicted.

Moreover, in Ref. [19], the nonlinear normal modes of an oscillating 2-DOF system with non-smooth piecewise linear characteristics which are considered to model a beam with a breathing crack or a system colliding with an elastic obstacle are studied. The considered model having two discontinuity boundaries is non-linearizable and exhibits the peculiar feature of a number of nonlinear normal modes (*NNMs*) that are greater than the degrees of freedom of the system.

The main objective in the first part of this paper is to derive primarily the PDE of the beam's motion such that the concept of nonlinear normal modes is implemented. The obtained equations for the system under investigation are analyzed and solved using four different approximate-analytical methods known as the *method of Multiple Time Scales*, the *method of Normal Forms*, the *method of Shaw and Pierre* and the *method of King and Vakakis* [20–24]. A parametric study is carried out, using *MTS* method. So, the effect of the various physical and geometrical parameters of the mathematical model on the nonlinear response of the beam is evaluated. In particular, the relation between the nonlinear natural frequencies and the vibration amplitude is scrutinized. Moreover, the effect of changes on stiffness values of linear and cubic nonlinear parts of elastic foundation and the value of the compressive axial load on the linear and nonlinear dynamic response of the beam are studied.

In the second part of this study, the dynamic behavior and steady-state stability analyses of the system under investigation in the case of three-to-one internal resonance are investigated. The deflection time histories in the case of 3:1 internal resonance condition under variation of different parameters are obtained. Moreover, the surface plot of stable/unstable points of the results in the steady-state condition and the frequency response analysis are accordingly extracted.

Based on the above reviews, for a beam under compressive axial load resting on a nonlinear elastic foundation, it was noticed that so far no study has been distinctly reported on the nonlinear dynamic analysis using different nonlinear normal modes techniques and moreover, the study of steady-state stability analysis in the case of 3:1 internal resonance.

2 Derivation of governing equation of motion

A one-dimensional simply supported Euler–Bernoulli beam of finite length l resting on a nonlinear elastic

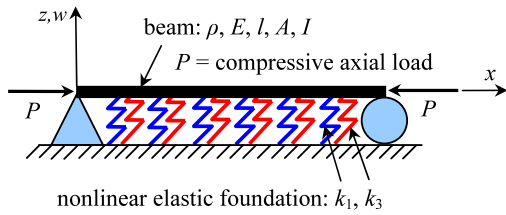


Fig. 1 A uniform hinged-hinged axially loaded beam resting on a nonlinear elastic foundation

foundation is shown in Fig. 1. As is seen from the figure, the beam is under a compressive axial load of P at its both ends. The nonlinear governing PDE of motion (EOM) of the beam is [13]:

$$\rho A w_{,tt} + EI w_{,xxxx} + P w_{,xx} + k_1 w + k_3 w^3 = 0 \quad (1)$$

in which $w = w(x, t)$ is the time-dependent transverse deflection of the beam measured upwards from its equilibrium position, the subscripts $(,t)$ and $(,x)$ stand for the derivative with respect to the time (t) and spatial coordinate (x) to the related order, respectively. Also, ρ is the beam density, A is the cross-sectional area of the beam, I is the beam's cross-sectional second moment of inertia, E is Young's modulus, EI is the beam's flexural rigidity which is constant along the beam's length, and ρA is the beam's mass per unit length. Moreover, k_1 and k_3 are the linear and cubic nonlinear parts of the elastic foundation stiffness (please see [13]). Moreover, boundary conditions (BCs) at both ends of the beam are

$$w = w_{,xx} = 0 \quad \text{at } x = 0 \text{ and } x = l. \quad (2)$$

To make upcoming analysis more convenient, the following dimensionless variables are defined:

$$\begin{aligned} x^* &= \frac{x}{l}, & t^* &= \frac{r_g}{l^2} \sqrt{\frac{E}{\rho}} t, & w^* &= \frac{w}{l}, \\ r_g^* &= \frac{r_g}{l}, & P^* &= \frac{Pl^2}{r_g^2 EA}, & k_1^* &= \frac{k_1 l^4}{r_g^2 EA}, \\ k_3^* &= \frac{k_3 l^6}{r_g^2 EA} \end{aligned} \quad (3)$$

where r_g is the radius of gyration of the beam's cross section. Substituting these dimensionless quantities into Eqs. (1) and (2) we obtain

$$w_{,t^*t^*}^* + w_{,x^*x^*x^*x^*}^* + P^* w_{,x^*x^*}^* + k_1^* w^* + k_3^* w^{*3} = 0, \quad (4a)$$

$$w^* = w_{,x^*x^*}^* = 0 \quad \text{at } x^* = 0 \text{ and } x^* = 1. \quad (4b)$$

By dropping the asterisks, one can rewrite Eqs. (4a) and (4b) as

$$w_{,tt} + w_{,xxxx} + P w_{,xx} + k_1 w + k_3 w^3 = 0, \quad (5)$$

$$w = w_{,xx} = 0 \quad \text{at } x = 0 \text{ and } x = 1. \quad (6)$$

In order to study the effect of nonlinear stiffness term, i.e., k_3 in response of the system, we introduce a non-dimensional multiplying parameter ϵ into Eq. (5), as [13, 20, 21]

$$w_{,tt} + w_{,xxxx} + P w_{,xx} + k_1 w + \epsilon k_3 w^3 = 0. \quad (7)$$

It is clear that, if $\epsilon = 0$, one deals with linear system and in the case of $\epsilon = 1$, the system is behaving as fully nonlinear. In subsequent sections, we try to solve Eq. (7) under boundary conditions of Eq. (6), using four different *nonlinear normal modes (NNMs)* methods.

3 Dynamic response with no 3:1 internal resonance [20–24]

3.1 Solution method 1: the method of Multiple Time Scales (MTS method)

In this method we seek a two-term two-time expansion of the solution for both Eqs. (6) and (7) using the following form:

$$w(x, t; \epsilon) = w_0(x, T_0, T_1) + \epsilon w_1(x, T_0, T_1) + O(\epsilon^2) \quad (8)$$

where $T_0 = t, T_1 = \epsilon t$ and $T_n = \epsilon^n t$ ($n = 0, 1, \dots$). Moreover, the first and second time derivatives in the dimensionless time domain become

$$\begin{aligned} \frac{\partial}{\partial t} &= \frac{\partial}{\partial T_0} + \epsilon \frac{\partial}{\partial T_1} + \dots \equiv D_0 + \epsilon D_1 + \epsilon^2 D_2 + \dots, \\ \text{and} \\ \frac{\partial^2}{\partial t^2} &= \frac{\partial^2}{\partial T_0^2} + 2\epsilon \frac{\partial^2}{\partial T_0 \partial T_1} + \dots \\ &\equiv D_0^2 + 2\epsilon D_0 D_1 + \epsilon^2 (2D_0 D_1 + D_1^2) + \dots, \end{aligned} \quad (9)$$

in which $D_n = \frac{\partial}{\partial T_n}$ with $n = 0, 1, \dots$. Substituting Eqs. (8) and (9) into Eqs. (6) and (7), then equating coefficients of the like powers of ε , we obtain:

for order ε^0 :

$$D_0^2 w_0 + w_0^{iv} + P w_0'' + k_1 w_0 = 0, \tag{10}$$

$$w_0 = w_0'' = 0 \quad \text{at } x = 0 \text{ and } x = 1, \tag{11}$$

for order ε^1 :

$$D_0^2 w_1 + w_1^{iv} + P w_1'' + k_1 w_1 = -2D_0 D_1 w_0 - k_3 w_0^3, \tag{12}$$

$$w_1 = w_1'' = 0 \quad \text{at } x = 0 \text{ and } x = 1, \tag{13}$$

in which the prime over any parameter denotes the derivative with respect to dimensionless variable parameter x to the related order. Now, to obtain the solution for nonlinear mode, we primarily begin with a linear solution for the m th linear mode by setting $\varepsilon \rightarrow 0$. It is obvious that at this stage one obtains the solution of zeroth-order linear problem (ε^0) as

$$w_0(x, T_0, T_1) = \sqrt{2} [A_m(T_1) e^{i\omega_m T_0} + \bar{A}_m(T_1) e^{-i\omega_m T_0}] \sin(m\pi x) \tag{14}$$

in which $i = \sqrt{-1}$, $A_m(T_1)$ and $\bar{A}_m(T_1)$ are two constant complex conjugates and expression $\sqrt{2} \sin(m\pi x)$ is the mode shape of vibration for a simply supported beam. Moreover, the corresponding linear circular frequency is given by

$$\omega_m^2 = k_1 + m^4 \pi^4 - P m^2 \pi^2 \quad \text{with } m = 1, 2, 3, \dots \tag{15}$$

Substituting Eq. (14) into the first-order Eq. (12) yields

$$\begin{aligned} D_0^2 w_1 + w_1^{iv} + P w_1'' + k_1 w_1 &= -2\sqrt{2} i \omega_m A_m'(T_1) e^{i\omega_m T_0} \sin(m\pi x) \\ &\quad - 2\sqrt{2} k_3 [A_m^3(T_1) e^{3i\omega_m T_0} \\ &\quad + 3A_m^2(T_1) \bar{A}_m(T_1) e^{i\omega_m T_0}] \sin^3(m\pi x) + \text{C.C.} \end{aligned} \tag{16}$$

where C.C. stands for a complex term in conjunction with other terms in Eq. (16). In addition, the prime on the RHS of Eq. (16) indicates the derivative with

respect to T_1 . To determine the solution for the case of the first-order (ε^1) problem, we consider

$$w_1(x, T_0, T_1) = g_1(x, T_1) e^{3i\omega_m T_0} + g_2(x, T_1) e^{i\omega_m T_0} + \text{C.C.} \tag{17}$$

By substituting Eq. (17) into Eq. (16), one can then equate the coefficients of $\exp(3i\omega_m T_0)$ and $\exp(i\omega_m \times T_0)$, respectively, on both sides to get

the coefficient of $\exp(3i\omega_m T_0)$:

$$\begin{aligned} g_1^{iv} + P g_1'' + (k_1 - 9\omega_m^2) g_1 &= -2\sqrt{2} k_3 A_m^3(T_1) \sin^3(m\pi x), \end{aligned} \tag{18}$$

$$g_1 = g_1'' = 0 \quad \text{at } x = 0 \text{ and } x = 1, \tag{19}$$

and the coefficient of $\exp(i\omega_m T_0)$:

$$\begin{aligned} g_2^{iv} + P g_2'' + (k_1 - \omega_m^2) g_2 &= -2\sqrt{2} i \omega_m A_m'(T_1) \sin(m\pi x) \\ &\quad - 6\sqrt{2} k_3 A_m^2(T_1) \bar{A}_m(T_1) \sin^3(m\pi x), \end{aligned} \tag{20}$$

$$g_2 = g_2'' = 0 \quad \text{at } x = 0 \text{ and } x = 1. \tag{21}$$

The solution of Eqs. (18) and (19) is given by

$$\begin{aligned} g_1(x, T_1) &= \frac{3\sqrt{2} k_3}{16\omega_m^2} A_m^3(T_1) \sin(m\pi x) \\ &\quad + \frac{\sqrt{2} k_3}{16(9m^4 \pi^4 - k_1)} A_m^3(T_1) \sin(3m\pi x). \end{aligned} \tag{22}$$

It is clear that the homogeneous part of Eqs. (20) and (21) has a nontrivial solution. On the other hand, the particular solution of Eqs. (20) and (21) exists only if a solvability condition is satisfied. In this case, the solvability condition demands that the right-hand side of Eq. (20) be orthogonal to the $\sin(m\pi x)$ which is the solution for the homogeneous problem. Hence, the solvability condition yields

$$2i\omega_m A_m'(T_1) = -\frac{9}{2} k_3 A_m^2(T_1) \bar{A}_m(T_1), \tag{23}$$

where the amplitude $A_m(T_1)$ in polar form is defined by

$$A_m(T_1) = \frac{1}{2} a_m(T_1) e^{i\beta_m(T_1)}. \tag{24}$$

Substituting the above into Eq. (23) and separating real and imaginary parts we obtain

$$a_m(T_1) = \text{const.} \quad \text{and} \quad \beta_m(T_1) = \frac{9k_3}{16\omega_m} a_m^2(T_1) T_1, \tag{25}$$

with $m = 1, 2, \dots, n$.

Then, the final solution of Eqs. (20) and (21) yields

$$g_2(x, T_1) = \frac{3\sqrt{2}k_3}{16(10m^4\pi^4 - Pm^2\pi^2)} \times A_m^2(T_1) \bar{A}_m(T_1) \sin(3m\pi x). \tag{26}$$

By substituting g_1 and g_2 into Eq. (17) one will obtain the solution for w_1 . Having on hand the solution for w_0 and w_1 , one can substitute them into Eq. (8) and then, by setting $\varepsilon = 1$, the expression for the transverse vibration deflection of the beam to the second order becomes

$$\begin{aligned} w(x, t) = & \sqrt{2}A_m(T_1) \sin(m\pi x) e^{i\omega_m t} \\ & + \frac{3\sqrt{2}k_3}{16(10m^4\pi^4 - Pm^2\pi^2)} \\ & \times A_m^2(T_1) \bar{A}_m(T_1) \sin(3m\pi x) e^{i\omega_m t} \\ & + \frac{\sqrt{2}k_3}{16} \left(\frac{3}{\omega_m^2} \sin(m\pi x) \right. \\ & \left. + \frac{1}{9m^4\pi^4 - k_1} \sin(3m\pi x) \right) \\ & \times A_m^3(T_1) e^{3i\omega_m t} + \text{C.C.} + \dots \end{aligned} \tag{27}$$

It follows from Eqs. (23) and (27) that the nonlinear natural frequencies $(\omega_{NL})_m$ of the beam's oscillation of the m th nonlinear mode can be given by

$$(\omega_{NL})_m = \omega_m \left(1 + \frac{9k_3}{16\omega_m^2} a_m^2 \right) + \dots \tag{28}$$

In the next step we try to determine the values of critical compressive axial loads out of $w(x, t)$ expression, i.e. Eq. (27). It becomes clear that if the denominator of the second term on the RHS in $w(x, t)$ expression approaches zero, i.e. $w(x, t) \rightarrow \infty$, this leads us to determine the value of critical compressive axial load of $P_{cr} = 10m^2\pi^2$ with $m = 1, 2, \dots, n$. Furthermore, we have the similar condition if the denominator of the fourth term on the RHS in $w(x, t)$ expression approaches zero, that is, if $9m^4\pi^4 - k_1 \rightarrow 0$, or

$k_1 = 9m^4\pi^4$ ($m = 1, 2, \dots, n$). This condition corresponds to the case of 3:1 internal resonance; in other words, in this condition it can be easily proven that $\omega_{3m} = 3\omega_m$ which is called a three-to-one internal resonance. In this case, there is a strong coupling between both the m th and $3m$ th modes and neither of them can be activated without activating the other one.

3.2 Solution method 2: the method of Normal Forms (NFs method)

The general form of the nonlinear partial-differential equation of the beam's motion, i.e., Eq. (5), can be expressed in the following form:

$$\ddot{w} + L(w) + N(w, \dot{w}, \ddot{w}) = 0 \tag{29}$$

where in our case $L(w) = w^{iv} + Pw'' + k_1w$ and $N(w, \dot{w}, \ddot{w}) = k_3w^3$. In this way the boundary conditions, i.e., Eq. (6), are

$$B(w) + BN(w, \dot{w}, \ddot{w}) = 0 \tag{30}$$

where the overdot indicates the derivative with respect to t , and in general L and B are linear spatial operators, and N and BN are nonlinear spatial and temporal operators of degree three, respectively. It should be noted that in our problem, $BN \equiv 0$. We implement an invariant manifold for Eqs. (29) and (30) that suggests the following solution for the motion m th normal mode where in this way the nonlinear nature of equations are converted to the linear behavior:

$$\begin{aligned} w(x, t) = & w(x, \zeta_m(t), \bar{\zeta}_m(t)) \\ = & (\zeta_m(t) + \bar{\zeta}_m(t)) \phi_m(x) \\ & + W(x, \zeta_m(t), \bar{\zeta}_m(t)). \end{aligned} \tag{31}$$

It should be noted that the first and second terms in the RHS of the above relation correspond to the solution of the linear and nonlinear parts, respectively. It further should be noted that the $\phi(x)$ in Eq. (31) represents the normal mode shape of simply supported beam, that is, $\phi_m(x) = \sqrt{2} \sin(m\pi x)$. It has been proved that the nature of the second term in Eq. (31) is cubic, therefore $W(x, \zeta_m, \bar{\zeta}_m)$ can be approximated by

$$\begin{aligned} W(x, \zeta_m(t), \bar{\zeta}_m(t)) = & f_1(x) (\zeta_m^3(t) + \bar{\zeta}_m^3(t)) + f_2(x) (\zeta_m^2(t) \bar{\zeta}_m(t) \\ & + \zeta_m(t) \bar{\zeta}_m^2(t)) + \text{H.O.T.} \end{aligned} \tag{32}$$

where H.O.T. stands for terms that are of the fourth or higher order in $\zeta_m(t)$ and $\bar{\zeta}_m(t)$. Moreover, it has to be emphasized that in any way W in Eq. (32) should yield a real value. In addition, the dynamics on this manifold is governed by

$$\dot{\zeta}_m(t) = i\omega_m \zeta_m(t) + h_m(\zeta_m(t), \bar{\zeta}_m(t)) \tag{33}$$

with

$$h_m(\zeta_m(t), \bar{\zeta}_m(t)) = \Gamma_m \zeta_m^2(t) \bar{\zeta}_m(t), \tag{34}$$

in which Γ_m is an unknown coefficient to be determined.

Having on hand the general solution for W , its second derivative can be calculated as

$$\begin{aligned} \frac{\partial^2 w}{\partial t^2} = & -\omega_m^2(\zeta_m + \bar{\zeta}_m)\phi_m(x) - \omega_m^2 \zeta_m^2 \frac{\partial^2 W}{\partial \zeta_m^2} \\ & + 2\omega_m^2 \zeta_m \bar{\zeta}_m \frac{\partial^2 W}{\partial \zeta_m \partial \bar{\zeta}_m} \\ & - \omega_m^2 \bar{\zeta}_m^2 \frac{\partial W}{\partial \bar{\zeta}_m} - \omega_m^2 \zeta_m \frac{\partial W}{\partial \zeta_m} - \omega_m^2 \bar{\zeta}_m \frac{\partial W}{\partial \bar{\zeta}_m} \\ & + 2i\omega_m(\Gamma_m \zeta_m^2 \bar{\zeta}_m - \bar{\Gamma}_m \bar{\zeta}_m^2 \zeta_m)\phi_m(x) + \text{H.O.T.} \end{aligned} \tag{35}$$

Substituting Eq. (35) into Eq. (5) and noting that $\omega_m = k_1 + m^4\pi^4 - Pm^2\pi^2$, after some mathematical simplifications one gets

$$\begin{aligned} W^{iv} + PW'' + k_1W - \omega_m^2 \zeta_m^2 \frac{\partial^2 W}{\partial \zeta_m^2} \\ + 2\omega_m^2 \zeta_m \bar{\zeta}_m \frac{\partial^2 W}{\partial \zeta_m \partial \bar{\zeta}_m} - \omega_m^2 \bar{\zeta}_m^2 \frac{\partial^2 W}{\partial \bar{\zeta}_m^2} \\ - \omega_m^2 \zeta_m \frac{\partial W}{\partial \zeta_m} - \omega_m^2 \bar{\zeta}_m \frac{\partial W}{\partial \bar{\zeta}_m} \\ + 2\sqrt{2}k_3(\zeta_m + \bar{\zeta}_m)^3 \sin^3(m\pi x) \\ + 2\sqrt{2}i\omega_m(\Gamma_m \zeta_m^2 \bar{\zeta}_m - \bar{\Gamma}_m \bar{\zeta}_m^2 \zeta_m) \sin(m\pi x) \\ + \dots = 0. \end{aligned} \tag{36}$$

Similarly for the boundary condition, that is, Eq. (6) in conjunction with Eq. (31), we have

$$W = W'' = 0 \quad \text{at } x = 0 \text{ and } x = 1. \tag{37}$$

Now, by substituting Eq. (32) into Eqs. (36) and (37) and equating the corresponding coefficients of $\zeta_m^3(t)$ and $\zeta_m^2(t)\bar{\zeta}_m(t)$ on both sides, we obtain:

the coefficient of $\zeta_m^3(t)$:

$$f_1^{iv} + Pf_1'' + (k_1 - 9\omega_m^2)f_1 = -2\sqrt{2}k_3 \sin^3(m\pi x), \tag{38}$$

$$f_1 = f_1'' = 0 \quad \text{at } x = 0 \text{ and } x = 1, \tag{39}$$

the coefficient of $\zeta_m^2(t)\bar{\zeta}_m(t)$:

$$\begin{aligned} f_2^{iv} + Pf_2'' + (k_1 - \omega_m^2)f_2 \\ = -2\sqrt{2}i\omega_m \Gamma_m \sin(m\pi x) - 6\sqrt{2}k_3 \sin^3(m\pi x), \end{aligned} \tag{40}$$

$$f_2 = f_2'' = 0 \quad \text{at } x = 0 \text{ and } x = 1. \tag{41}$$

The solution of Eqs. (38) and (39) yields

$$\begin{aligned} f_1(x) = & \frac{3\sqrt{2}k_3}{16\omega_m^2} \sin(m\pi x) \\ & + \frac{\sqrt{2}k_3}{16(9m^4\pi^4 - k_1)} \sin(3m\pi x). \end{aligned} \tag{42}$$

It can be easily verified that the nontrivial solution for Eqs. (40) and (41) exists if the following condition prevails:

$$2i\omega_m \Gamma_m = -\frac{9}{2}k_3. \tag{43}$$

Then, the solution for $f_2(x)$ accordingly yields

$$f_2(x) = \frac{3\sqrt{2}k_3}{16(10m^4\pi^4 - Pm^2\pi^2)} \sin(3m\pi x). \tag{44}$$

Now, having on hand the solutions for $f_1(x)$ and $f_2(x)$, one can obtain the final solution for the nonlinear normal mode:

$$\begin{aligned} w(x, t) = & \sqrt{2}(\zeta_m(t) + \bar{\zeta}_m(t)) \sin(m\pi x) \\ & + \frac{3\sqrt{2}k_3}{16(10m^4\pi^4 - Pm^2\pi^2)} (\zeta_m^2(t)\bar{\zeta}_m(t) \\ & + \zeta_m(t)\bar{\zeta}_m^2(t)) \sin(3m\pi x) \\ & + \frac{\sqrt{2}k_3}{16} (\zeta_m^3(t) + \bar{\zeta}_m^3(t)) \left(\frac{3}{\omega_m^2} \sin(m\pi x) \right. \\ & \left. + \frac{1}{9m^4\pi^4 - k_1} \sin(3m\pi x) \right) + \dots \end{aligned} \tag{45}$$

To determine the dynamics on the nonlinear normal mode, we substitute the calculated value for the Γ_m

into Eq. (34), and the obtained result into Eq. (33):

$$\dot{\zeta}_m(t) = i\omega_m \zeta_m(t) + \frac{9ik_3}{4\omega_m} \zeta_m^2(t) \bar{\zeta}_m(t). \tag{46}$$

By a close inspection of Eqs. (45) and (46) it becomes clear that if we replace $\zeta_m(t)$ with $A_m \exp(i\omega_m t)$, the results yield exactly Eqs. (23) and (27), in which the *MTS* method has been utilized. Again, Eq. (45) becomes independently singular if $k_1 = 9m^4\pi^4$ or $P_{cr} = 10m^2\pi^2$ with $m = 1, 2, \dots, n$, indicating the cases of the *three-to-one internal resonance* and the *critical compressive axial load* of the beam, respectively.

3.3 Solution method 3: the method of Shaw and Pierre (S&P method)

Based on the methodology presented by *Shaw and Pierre*, one can express Eq. (29) as a system of two partial-differential equations; that is,

$$\dot{w} = v, \tag{47}$$

$$\dot{v} = -L(w) - N[w, v]. \tag{48}$$

In their proposed method, if $w_0(t)$ and $v_0(t)$ represent the displacement and velocity of the system at an arbitrary reference point of $x = x_0$, then for an equilibrium point one can establish $[w(x_0, t), v(x_0, t)] = [0, 0]$. Furthermore, this reference position should not be taken over any nodal point associated with the non-linear mode. Then, the entire displacement and velocity fields can be expressed in terms of the dynamics of the reference point x_0 as [20, 21]:

$$w(x, t) = W(x, x_0, w_0(t), v_0(t)), \tag{49a}$$

$$v(x, t) = V(x, x_0, w_0(t), v_0(t)). \tag{49b}$$

Based on this technique, the set of independent variables (x, t) is changed to $(x, w_0(t), v_0(t))$ and, accordingly, the explicit dependence on t will be eliminated. Consequently, in the new domain and at equilibrium condition, Eqs. (49a) and (49b) will change to

$$w_0(x_0, t) = W(x_0, x_0, w_0(t), v_0(t)), \tag{50a}$$

$$v_0(x_0, t) = V(x_0, x_0, w_0(t), v_0(t)). \tag{50b}$$

In general, Eqs. (50a) and (50b) are known as the *compatibility conditions*. Moreover, it follows from

Eqs. (47)–(50a), (50b) that the dynamics of the non-linear normal mode is

$$\dot{w}_0 = v_0, \tag{51}$$

$$\dot{v}_0 = -[L(W) + N(W, V)]_{x=x_0}. \tag{52}$$

In order to convert the general form of the beam’s PDE of motion, i.e., Eq. (29), we begin with differentiation of Eqs. (49a), (49b) with respect to t :

$$\dot{w}(x, t) = \frac{\partial W}{\partial w_0} \dot{w}_0 + \frac{\partial W}{\partial v_0} \dot{v}_0 \quad \text{and}$$

$$\dot{v}(x, t) = \frac{\partial V}{\partial w_0} \dot{w}_0 + \frac{\partial V}{\partial v_0} \dot{v}_0.$$

By combining Eqs. (47), (48), (51) and (52), one would get the functional equations as

$$\frac{\partial W}{\partial w_0} v_0 - \frac{\partial W}{\partial v_0} [L(W) + N(W, V)]_{x=x_0} = V, \tag{53}$$

$$\begin{aligned} \frac{\partial V}{\partial w_0} v_0 - \frac{\partial V}{\partial v_0} [L(W) + N(W, V)]_{x=x_0} \\ = -L(W) - N[W, V]. \end{aligned} \tag{54}$$

Similarly, for the boundary conditions we have

$$B(W) + BN[W, V, -L(W) - N(W, V)] = 0. \tag{55}$$

Now, in our problem we can substitute the form of $L(w) = w^{iv} + Pw'' + k_1w$ and $N(w, v) = k_3w^3$ operators into Eqs. (53) to (54), which yields the following functional equations:

$$\begin{aligned} \frac{\partial W}{\partial w_0} v_0 - \frac{\partial W}{\partial v_0} [W^{iv} + PW'' + k_1W + k_3W^3]_{x=x_0} \\ = V, \end{aligned} \tag{56}$$

$$\begin{aligned} \frac{\partial V}{\partial w_0} v_0 - \frac{\partial V}{\partial v_0} [W^{iv} + PW'' + k_1W + k_3W^3]_{x=x_0} \\ = -W^{iv} - PW'' - k_1W - k_3W^3, \end{aligned} \tag{57}$$

and the corresponding boundary conditions become

$$W = W'' = 0 \quad \text{at } x = 0 \text{ and } x = 1. \tag{58}$$

To solve Eqs. (56)–(58) subject to the compatibility conditions, i.e., Eqs. (50a) and (50b), we use the expanded form of W and V in terms of $w_0(t)$ and $v_0(t)$ as following:

$$\begin{aligned} W = a_1(x, x_0)w_0(t) + a_2(x, x_0)w_0^3(t) \\ + a_3(x, x_0)w_0(t)v_0^2(t) + \dots, \end{aligned} \tag{59}$$

$$V = b_1(x, x_0)v_0(t) + b_2(x, x_0)w_0^2(t)v_0(t) + b_3(x, x_0)v_0^3(t) + \dots \tag{60}$$

Noting that the above solutions should satisfy the compatibility conditions, Eqs. (50a) and (50b), thus

$$a_1(x_0, x_0) = 1, \quad b_1(x_0, x_0) = 1, \tag{61}$$

$$a_i(x_0, x_0) = 0, \quad b_i(x_0, x_0) = 0 \quad \text{for } i \geq 2.$$

And by forcing the boundary conditions equation (58) on Eqs. (59) and (60), one gets

$$a_i(x, x_0) = a_i''(x, x_0) = 0 \quad \text{at } x = 0 \text{ and } x = 1. \tag{62}$$

The rest of the unknown variable coefficients of a_i 's and b_i 's can be obtained by equating the coefficients of the like powers of $w_0^m v_0^n$, in Eqs. (56)–(57) and using the compatibility conditions, Eq. (61), which yields:

the coefficient of v_0 :

$$b_1(x, x_0) = a_1(x, x_0), \tag{63}$$

the coefficient of w_0 :

$$a_1^{iv}(x, x_0) - a_1^{iv}(x_0, x_0)a_1(x, x_0) - Pa_1(x, x_0)a_1''(x_0, x_0) + Pa_1''(x, x_0) = 0, \tag{64}$$

the coefficient of $w_0^2 v_0$:

$$b_2(x, x_0) = 3a_2(x, x_0) - 2[k_1 a_1(x_0, x_0) + a_1^{iv}(x_0, x_0) + Pa_1''(x_0, x_0)]a_3(x, x_0), \tag{65}$$

the coefficient of v_0^3 :

$$b_3(x, x_0) = a_3(x, x_0), \tag{66}$$

the coefficient of $w_0^2 v_0^2$:

$$2b_2(x, x_0) - Pb_1(x, x_0)a_3''(x_0, x_0) - 3Pb_3(x, x_0)a_1''(x_0, x_0) = a_3^{iv}(x_0, x_0)a_1(x, x_0) - a_3^{iv}(x, x_0) - k_1 a_3(x, x_0) + 3[k_1 a_1(x_0, x_0) + a_1^{iv}(x_0, x_0)]a_3(x, x_0) - Pa_3''(x, x_0), \tag{67}$$

the coefficient of w_0^3 :

$$a_2^{iv}(x, x_0) - a_2^{iv}(x_0, x_0)a_1(x, x_0) + Pa_2''(x, x_0) + k_1 a_2(x, x_0) - [k_1 a_1(x_0, x_0)$$

$$+ a_1^{iv}(x_0, x_0)]b_2(x, x_0) - Pb_2(x, x_0)a_1''(x_0, x_0) - Pb_1(x, x_0)a_2''(x_0, x_0) = k_3[a_1(x, x_0)a_1^3(x_0, x_0) - a_1^3(x, x_0)]. \tag{68}$$

The solution of Eq. (64) subject to the compatibility and boundary conditions equations (61) and (62) is

$$a_1(x, x_0) = \frac{\sin(m\pi x)}{\sin(m\pi x_0)} \quad \text{with } m = 1, 2, 3, \dots \tag{69}$$

Having on hand $a_1(x, x_0)$, one can easily eliminate $b_2(x, x_0)$ and $a_1(x, x_0)$ from Eqs. (67) and (68) to obtain

$$a_2^{iv}(x, x_0) - a_2^{iv}(x_0, x_0) \frac{\sin(m\pi x)}{\sin(m\pi x_0)} - (2k_1 + 3m^4\pi^4 + 6m^2\pi^2 P)a_2(x, x_0) + 2(k_1 + m^4\pi^4 - m^2\pi^2 P)^2 a_3(x, x_0) = -k_3 \left[\frac{\sin^3(m\pi x)}{\sin^3(m\pi x_0)} - \frac{\sin(m\pi x)}{\sin(m\pi x_0)} \right], \tag{70}$$

$$a_3^{iv}(x, x_0) - a_3^{iv}(x_0, x_0) \frac{\sin(m\pi x)}{\sin(m\pi x_0)} - (6k_1 + 7m^4\pi^4 + 2m^2\pi^2 P)a_3(x, x_0) + 6a_2(x, x_0) = 0. \tag{71}$$

Again, we seek the solution of Eqs. (70) and (71) that satisfies the compatibility and boundary conditions equations (61) and (62) in the form [20, 21]:

$$a_2(x, x_0) = c_1 \left[\frac{\sin^3(m\pi x)}{\sin^3(m\pi x_0)} - \frac{\sin(m\pi x)}{\sin(m\pi x_0)} \right], \tag{72}$$

$$a_3(x, x_0) = c_2 \left[\frac{\sin^3(m\pi x)}{\sin^3(m\pi x_0)} - \frac{\sin(m\pi x)}{\sin(m\pi x_0)} \right].$$

Differentiating Eq. (72) up to four times with respect to x , one can find that

$$a_i^{iv}(x, x_0) - a_i^{iv}(x_0, x_0) \frac{\sin(m\pi x)}{\sin(m\pi x_0)} = 81m^4\pi^4 a_i(x, x_0) \quad \text{for } i = 2, 3 \quad \text{and} \tag{73}$$

$$a_i''(x, x_0) - a_i''(x_0, x_0) \frac{\sin(m\pi x)}{\sin(m\pi x_0)} = -9m^2\pi^2 a_i(x, x_0) \quad \text{for } i = 2, 3.$$

Substituting Eq. (72) into Eqs. (70) and (71) and using Eq. (73), we obtain

$$\begin{aligned} (78m^4\pi^4 - 2k_1 - 6m^2\pi^2P)c_1 \\ + 2(k_1 + m^4\pi^4 - m^2\pi^2P)^2c_2 = -k_3, \quad (74) \\ 6c_1 + (74m^4\pi^4 - 6k_1 - 2m^2\pi^2P)c_2 = 0, \end{aligned}$$

whose solution yields

$$\begin{aligned} c_1 = \frac{(3k_1 - 37m^4\pi^4 + m^2\pi^2P)k_3}{32(9m^4\pi^4 - k_1)(10m^4\pi^4 - m^2\pi^2P)}, \quad (75) \\ c_2 = \frac{3k_3}{32(9m^4\pi^4 - k_1)(10m^4\pi^4 - m^2\pi^2P)}. \end{aligned}$$

After some mathematical manipulation and simplifications one can easily find the solutions for $a_2(x, x_0)$ and $a_3(x, x_0)$. Then, having on hand the final answer for $a_1(x, x_0)$, $a_2(x, x_0)$ and $a_3(x, x_0)$, the final solution for the nonlinear normal mode becomes

$$\begin{aligned} W = a_1(x, x_0)w_0(t) \\ + \frac{k_3}{32(9m^4\pi^4 - k_1)(10m^4\pi^4 - m^2\pi^2P)} \\ \times [(3k_1 - 37m^4\pi^4 + m^2\pi^2P)w_0^3(t) \\ + 3w_0(t)v_0^2(t)][a_1^3(x, x_0) - a_1(x, x_0)] + \dots \quad (76) \end{aligned}$$

Moreover, in order to have the solution of V , by back-substitution of obtained values of $a_1(x, x_0)$, $a_2(x, x_0)$ and $a_3(x, x_0)$ from Eqs. (69) and (72) into Eq. (65) and using the values of c_1 and c_2 , one gets

$$\begin{aligned} b_2(x, x_0) = \frac{3(k_1 - 39m^4\pi^4 + 3m^2\pi^2P)k_3}{32(9m^4\pi^4 - k_1)(10m^4\pi^4 - m^2\pi^2P)} \\ \times [a_1^3(x, x_0) - a_1(x, x_0)]. \quad (77) \end{aligned}$$

Substituting for $b_1(x, x_0)$, $b_2(x, x_0)$ and $b_3(x, x_0)$ into Eq. (60) yields

$$\begin{aligned} V = a_1(x, x_0)v_0(t) \\ + \frac{3k_3}{32(9m^4\pi^4 - k_1)(10m^4\pi^4 - m^2\pi^2P)} \\ \times [(k_1 - 39m^4\pi^4 + 3m^2\pi^2P)w_0^2(t)v_0(t) \\ + v_0^3(t)][a_1^3(x, x_0) - a_1(x, x_0)] + \dots \quad (78) \end{aligned}$$

It emerges from Eqs. (51), (52) and (5) that the dynamics of the nonlinear mode is given by

$$\ddot{w}_0 + [W^{iv} + PW'' + k_1W + k_3W^3]_{x=x_0} = 0 \quad (79)$$

which, upon using Eq. (76), becomes

$$\begin{aligned} \ddot{w}_0(t) + \omega_m^2w_0(t) - \frac{k_3}{16(9m^4\pi^4 - k_1)\sin^2(m\pi x_0)} \\ \times \{[3(3k_1 - 37m^4\pi^4 + m^2\pi^2P) \\ + 4\omega_m^2\sin^2(m\pi x_0)]w_0^3(t) \\ + 3[3 - 4\sin^2(m\pi x_0)]w_0(t)\dot{w}_0^2(t)\} + \dots = 0. \quad (80) \end{aligned}$$

After imposing the method of *MTS* mentioned in Sect. 3.1 to Eq. (80), we primarily have to begin with an initial solution for $w_0(T_0, T_1)$, leading us to the final solution. It can be proven that this initial solution will be in the form of $w_0(T_0, T_1) = \varepsilon w_1(T_0, T_1) + \varepsilon^3 w_3(T_0, T_1) + \dots$. Having on hand this primary solution, we then can substitute it into Eq. (80) and then, by separating the first-order (ε^1) and third-order (ε^3) of perturbation levels, one respectively yields $w_1(T_0, T_1) = B_m(T_1)e^{i\omega_m T_0} + C.C.$ and $w_3(T_0, T_1) = K_m(T_1)e^{3i\omega_m T_0} + C.C.$ By back-substitution of the obtained results for $w_1(T_0, T_1)$ and $w_3(T_0, T_1)$ into $w_0(T_0, T_1)$ relation and the result into Eq. (80), now we can impose condition of $\varepsilon = 1$. In the next step we equate the coefficient of $\exp(3i\omega_m T_0)$ on both sides of the result to obtain the final solution for the amplitude $K_m(T_1)$ in terms of $B_m(T_1)$. Then finally $w_0(T_0, T_1)$ becomes

$$\begin{aligned} w_0(t) \\ = B_m(T_1)e^{i\omega_m T_0} \\ + \frac{k_3[15m^4\pi^4 - \frac{3}{2}m^2\pi^2P - 2\omega_m^2\sin^2(m\pi x_0)]}{16\omega_m^2(9m^4\pi^4 - k_1)\sin^2(m\pi x_0)} \\ \times B_m^3(T_1)e^{3i\omega_m T_0} + C.C. + \dots \quad (81) \end{aligned}$$

where the solvability condition is given by

$$2i\omega_m B_m'(T_1) = -\frac{9k_3}{4\sin^2(m\pi x_0)}B_m^2(T_1)\bar{B}_m(T_1), \quad (82)$$

in which the amplitude $B_m(T_1)$ in polar form is defined by $B_m(T_1) = \frac{1}{2}b_m(T_1)e^{i\gamma_m(T_1)}$. Substituting this relation for $B_m(T_1)$ into Eq. (82) and separating real and imaginary parts, one obtains $b_m(T_1) =$

const. and $\gamma_m(T_1) = \frac{9k_3}{32\omega_m \sin^2(m\pi x_0)} b_m^2(T_1) T_1$, with $m = 1, 2, \dots, n$.

Substituting Eq. (81) into Eq. (76) and using Eq. (51), one gets

$$\begin{aligned}
 W = \sin(m\pi x) & \left[\frac{B_m(T_1)}{\sin(m\pi x_0)} - \frac{3k_3[3 - 4\sin^2(m\pi x_0)]}{320m^4\pi^4 \sin^3(m\pi x_0)} \right. \\
 & \times B_m^2(T_1) \bar{B}_m(T_1) \left. \right] e^{i\omega_m T_0} \\
 & + \frac{3k_3}{32(10m^4\pi^4 - m^2\pi^2 P) \sin^3(m\pi x_0)} \\
 & \times B_m^2(T_1) \bar{B}_m(T_1) \sin(3m\pi x) e^{i\omega_m T_0} \\
 & + \frac{k_3}{32} \left[\frac{3}{\omega_m^2} \sin(m\pi x) \right. \\
 & \left. + \frac{1}{9m^4\pi^4 - k_1} \sin(3m\pi x) \right] \frac{B_m^3(T_1)}{\sin^3(m\pi x_0)} e^{3i\omega_m T_0} \\
 & + \text{C.C.} + \dots \tag{83}
 \end{aligned}$$

Now, if we take the expression given in the first bracket at the RHS of Eq. (83), i.e., $\frac{B_m(T_1)}{\sin(m\pi x_0)} - \frac{3k_3[3-4\sin^2(m\pi x_0)]}{320m^4\pi^4 \sin^3(m\pi x_0)} B_m^2(T_1) \bar{B}_m(T_1)$, and equal it to $\sqrt{2}A_m(T_1)$, then Eqs. (82) and (83) yield exactly the same form as was in Eqs. (23) and (27), respectively, in which the MTS method has been used. Again, it is clear that Eqs. (76) and (78) become independently singular if $k_1 = 9m^4\pi^4$ or $P_{cr} = 10m^2\pi^2$ with $m = 1, 2, \dots, n$, indicating the cases of the *three-to-one internal resonance* and the *critical compressive axial load* of the beam, respectively.

3.4 Solution method 4: the method of King and Vakakis (K&V method)

Based on the methodology presented by King and Vakakis, by specifying the displacement w_0 at the reference point x_0 , one can express the displacement field $w(x, t)$ in terms of $w_0(t)$ only because $v_0(t)$ can be expressed in terms of $w_0(t)$; that is,

$$w(x, t) = W(x, x_0, w_0(t)). \tag{84}$$

In this method, the set of independent variables (x, t) will change to $(x, w_0(t))$, where $w_0(t)$ can be thought of as a nonlinear time scale. Therefore, at a specific fixed point x_0 it follows from Eq. (84) that

$$w_0(x_0, t) = W(x_0, x_0, w_0(t)). \tag{85}$$

Equation (85) is usually called a compatibility condition. Once $W(x_0, x_0, w_0(t))$ is computed, the dynamics of the nonlinear normal mode can be found from Eq. (29) as

$$\ddot{w}_0 = -[L(W) + N(W)]_{x=x_0}. \tag{86}$$

Again, in order to convert the general form of the beam’s PDE of motion, Eq. (29), we begin with differentiation of Eq. (84) with respect to t to yield

$$\dot{w}(x, t) = \frac{\partial W}{\partial w_0} \dot{w}_0, \tag{87}$$

which, upon differentiation with respect to t , yields

$$\ddot{w} = \frac{\partial W}{\partial w_0} \ddot{w}_0 + \frac{\partial^2 W}{\partial w_0^2} \dot{w}_0^2. \tag{88}$$

In this method, by employing the principle of total energy and doing some mathematical simplifications, one gets [20, 21]:

$$\ddot{w}_0 + \omega_m^2 w_0 + \varepsilon f(w_0) = 0, \tag{89}$$

in which ω_m is the linear frequency of the m th normal mode and ε and $f(w_0) = N[W(x_0, x_0, w_0(t))]$ are a non-dimensional parameter and a nonlinear function, respectively defined as before. Hence [20, 21],

$$\frac{1}{2} \dot{w}_0^2 + \frac{1}{2} \omega_m^2 w_0^2 + \varepsilon F(w_0) = \frac{1}{2} \omega_m^2 w_0^{*2} + \varepsilon F(w_0^*), \tag{90}$$

in which w_0^* is the maximum of w_0 and $F'(w_0) = f(w_0)$. From Eq. (90), \dot{w}_0^2 can be easily found:

$$\dot{w}_0^2 = \omega_m^2 (w_0^{*2} - w_0^2) + 2\varepsilon F(w_0^*) - 2\varepsilon F(w_0). \tag{91}$$

By combining Eqs. (29), (86), (88) and (91), one yields the singular functional equation:

$$\begin{aligned}
 & \left[\omega_m^2 (w_0^{*2} - w_0^2) + 2\varepsilon F(w_0^*) - 2\varepsilon F(w_0) \right] \frac{\partial^2 W}{\partial w_0^2} \\
 & - [L(W) + N(W)]_{x=x_0} \frac{\partial W}{\partial w_0} \\
 & = -L(W) - N(W). \tag{92}
 \end{aligned}$$

Now, we can replace the expression $L(W) + N(W)$ in Eq. (92) by recalling Eq. (7). The result becomes

$$\begin{aligned}
 & [\omega_m^2(w_0^{*2} - w_0^2) + 2\varepsilon F(w_0^*) - 2\varepsilon F(w_0)] \frac{\partial^2 W}{\partial w_0^2} \\
 & - [W^{iv} + PW'' + k_1W + \varepsilon k_3W^3]_{x=x_0} \frac{\partial W}{\partial w_0} \\
 & = -W^{iv} - PW'' - k_1W - \varepsilon k_3W^3, \tag{93}
 \end{aligned}$$

subject to the boundary conditions given by Eq. (37). The solution of Eq. (93) using this method is given by an approximation to W in a power series of ε as [20, 21]:

$$W = a_1(x, x_0)w_0(t) + \varepsilon W_1(x, x_0, w_0(t)) + \dots, \tag{94}$$

in which $a_1(x, x_0)$ and $W_1(x, x_0, w_0)$ are unknown functions to be determined later. By applying the compatibility conditions on Eq. (94), we obtain

$$a_1(x_0, x_0) = 1 \quad \text{and} \quad W_1(x_0, x_0, w_0(t)) = 0. \tag{95}$$

Furthermore, by applying the boundary conditions given in Eq. (37) to Eq. (94), one gets

$$\begin{aligned}
 a_1 = a_1'' = 0 \quad \text{and} \quad W_1 = W_1'' = 0 \\
 \text{at } x = 0 \text{ and } x = 1. \tag{96}
 \end{aligned}$$

Now, in order to obtain a solution for W , we substitute Eq. (94) into Eqs. (93) and (37), out of which a general relation is derived. Then, in the first step of deriving complete solution for a_1 we equate the coefficient of ε^0 on both sides of this general relation, and then an ODE relation is obtained which can be solved simultaneously with the compatibility condition, i.e., Eq. (95). The final result at this stage becomes exactly the same as the one given in Eq. (64). The solution of Eq. (64) subject to the boundary and compatibility conditions in Eqs. (95) and (96) is given by Eq. (69) where ω_m is given by Eq. (15).

In the next step of deriving complete set of solutions for $W_1(x, x_0, w_0(t))$, by equating the coefficients of ε on both sides of the above general relation and using a similar technique as before, we obtain

$$\begin{aligned}
 & (k_1 + m^4\pi^4 - m^2\pi^2P)(w_0^{*2} - w_0^2) \frac{\partial^2 W_1}{\partial w_0^2} \\
 & - [W_1^{iv} + PW_1'' + k_1W_1 + k_3a_1^3w_0^3]_{x=x_0} a_1(x, x_0) \\
 & - a_1(x, x_0)(k_1 + m^4\pi^4 - m^2\pi^2P)w_0 \frac{\partial W_1}{\partial w_0} \\
 & = -W_1^{iv} - PW_1'' - k_1W_1 - k_3a_1^3(x, x_0)w_0^3. \tag{97}
 \end{aligned}$$

Solution of Eq. (97) for $W_1(x, x_0, w_0)$ is given by [20, 21]:

$$W_1(x, x_0, w_0(t)) = a_2(x, x_0)w_0(t) + a_3(x, x_0)w_0^3(t). \tag{98}$$

Equation (98), subject to constraint relations specified by Eqs. (95) and (96), and after equating coefficients of the like powers of $w_0(t)$ from both sides, yields the following results:

$$\begin{aligned}
 a_i(x_0, x_0) = 0 \quad \text{and} \quad a_i = a_i'' = 0 \\
 \text{at } x = 0 \text{ and } x = 1 \text{ for } i = 2 \text{ and } 3. \tag{99}
 \end{aligned}$$

Moreover, by substituting Eq. (98) into Eq. (97) and equating coefficients of the like powers of $w_0(t)$ from both sides, we have:

the coefficient of w_0^3 :

$$\begin{aligned}
 & a_3^{iv}(x, x_0) - a_3^{iv}(x_0, x_0)a_1(x, x_0) \\
 & - Pa_3''(x_0, x_0)a_1(x, x_0) + Pa_3''(x, x_0) \\
 & - (9k_1 + 9m^4\pi^4 - 9m^2\pi^2P)a_3(x, x_0) \\
 & + k_1a_3(x, x_0) = k_3[a_1(x, x_0) - a_1^3(x, x_0)], \tag{100}
 \end{aligned}$$

the coefficient of w_0 :

$$\begin{aligned}
 & a_2^{iv}(x, x_0) - a_2^{iv}(x_0, x_0)a_1(x, x_0) + Pa_2''(x, x_0) \\
 & - Pa_2''(x_0, x_0)a_1(x, x_0) \\
 & - (m^4\pi^4 - m^2\pi^2P)a_1(x_0, x_0)a_2(x, x_0) \\
 & = -6\omega_m^2w_0^{*2}a_3(x, x_0). \tag{101}
 \end{aligned}$$

We note that Eqs. (100) and (101) are uncoupled. Thus, one can solve for $a_3(x, x_0)$ first and then solve for $a_2(x, x_0)$. Note that the uncoupled Eqs. (100) and (101) can be obtained separately by considering the transformations $\psi_3 = a_3$ and $\psi_2 = a_2 - \omega_m^2\psi_3$ imposed on coupled Eqs. (70) and (71) which were derived by using the *method* of Shaw and Pierre. Still, one can transform the coupled Eqs. (70) and (71) to uncoupled equations other than the above method if instead of $a_2 - \omega_m^2a_3$ one uses a new dependent variable, say ψ_1 . In this way the final results become exactly the same as the ones obtained by the *method* of King and Vakakis.

To obtain the final solution for W , we seek for an answer to the Eqs. (100) and (101). To do this, we follow the same steps as described in deriving Eq. (76).

In other words, by considering Eq. (99) and substituting Eqs. (72) and (69) into Eqs. (100) and (101) along with Eq. (73), one primarily gets

$$\begin{aligned} (72m^4\pi^4 - 8k_1)c_2 &= -k_3, \\ (80m^4\pi^4 - 8m^2\pi^2P)c_1 &= -6\omega_m^2w_0^{*2}c_2 \end{aligned} \tag{102}$$

yielding the following answers for c_1 and c_2 :

$$\begin{aligned} c_1 &= \frac{3\omega_m^2k_3w_0^{*2}}{32(9m^4\pi^4 - k_1)(10m^4\pi^4 - m^2\pi^2P)} \quad \text{and} \\ c_2 &= -\frac{k_3}{8(9m^4\pi^4 - k_1)}. \end{aligned} \tag{103}$$

Then one gets the final answer for W as

$$\begin{aligned} W &= a_1(x, x_0)w_0(t) + \frac{k_3}{8(9m^4\pi^4 - k_1)} \\ &\times \left[\frac{3\omega_m^2}{4(10m^4\pi^4 - m^2\pi^2P)}w_0^{*2}(t)w_0(t) - w_0^3(t) \right] \\ &\times [a_1^3(x, x_0) - a_1(x, x_0)] + \dots \end{aligned} \tag{104}$$

Substituting Eq. (104) into Eq. (15), evaluating the result at $x = x_0$ and setting $\varepsilon = 1$, one gets the dynamics of the nonlinear mode as

$$\begin{aligned} \ddot{w}_0(t) + \omega_m^2w_0(t) + \frac{k_3}{2(9m^4\pi^4 - k_1)\sin^2(m\pi x_0)} \\ \times \left\{ \frac{3\omega_m^2}{8}[4\sin^2(m\pi x_0) - 3] \times w_0^{*2}(t)w_0(t) \right. \\ \left. + \left[\frac{3}{2}(10m^4\pi^4 - m^2\pi^2P) - 2\omega_m^2\sin^2(m\pi x_0) \right] w_0^3(t) \right\} + \dots = 0. \end{aligned} \tag{105}$$

Again, Eq. (104) becomes independently singular if $k_1 = 9m^4\pi^4$ or $P_{cr} = 10m^2\pi^2$ with $m = 1, 2, \dots, n$, indicating the cases of the *three-to-one internal resonance* and the *critical compressive axial load*, respectively.

Now, in deriving nonlinear normal modes (NNMs), we can qualitatively compare the outcomes of the above four different methods related to Eqs. (5) and (6). By comparison of the above four methods, the following preliminary conclusions are drawn:

- (i) If in Eqs. (45) and (46) we replace $\zeta_m(t)$ with $A_m(T_1)\exp(i\omega_m t)$, by a close inspection of obtained results using the *method of Normal Forms*

(*NFs method*) it becomes clear that the outcome yields exactly those obtained from the *method of Multiple Time Scales* (see Eqs. (23) and (27)).

- (ii) If we replace the first bracket of RHS of Eq. (83) with $\sqrt{2}A_m(T_1)$, the obtained results in Eqs. (82) and (83) using the *method of Shaw and Pierre* will turn exactly to the same expression as given in the *method of Multiple Time Scales (MTS)* (see Eqs. (23) and (27)).

- (iii) *Comparison of the S&P and K&V methods:*

- (iii-1) It can be proven that solution of Eq. (105) using the *MTS* method up to the second approximation yields the same result as in Eq. (81) derived by the *method of Shaw and Pierre* if $B'_m(T_1)$ is replaced by Eq. (82).

- (iii-2) Substituting Eq. (81) obtained by the *method of Shaw and Pierre* into Eq. (104) obtained by the *method of King and Vakkis*, considering $w_0^{*2}(t) = 4B_m(T_1)\bar{B}_m(T_1)$ yields the answer for the W which is the same as given in Eq. (83) obtained by the *method of Shaw and Pierre*. That is, by following the above steps the answer out of the fourth method yields the answer out of the third method.

- (iii-3) Conversely, we can replace $w_0^{*2}(t)$ with $w_0^2(t) + \omega_m^{-2}\dot{w}_0^2(t)$ in Eqs. (104) and (105) and arrive at the results given in Eqs. (76) and (80). That is, by following the above steps the answer out of the third method yields the answer out of the fourth method.

- (iv) *Interconnections of all the NNMs methods:*

Referred to all the above findings, it can be observed that the results obtained individually by each *method of K&V, S&P, MTS* and *NFs* become exactly the same if proper replacements or conversions between these methods are imposed.

It has to be observed that the final solution of the governing ODE of the beam's vibration, i.e., Eq. (5) under given boundary conditions in Eq. (6), using the above four nonlinear normal modes techniques yields the same answer. Now, in order to continue further in-depth investigation of the effect of different parameters on the beam's dynamics, we prefer to use the solution technique given by the *MTS* method.

4 Behavioral analysis in the case of 3:1 internal resonance

4.1 Dynamic response

In this section, to have a better insight of what happens in the presence of 3:1 internal resonance, i.e. $k_1 = 9m^4\pi^4$ ($m = 1, 2, \dots, n$), and to construct the nonlinear normal modes in this case using the MTS method, Eqs. (5) and (6) will be considered. Having on hand the results given in Eqs. (10) and (11), the zeroth-order solution in the case of 3:1 internal resonance with $n = 3m$ will be taken as

$$w_0(x, T_0, T_1) = \sqrt{2}A_m(T_1)e^{i\omega_m T_0} \sin(m\pi x) + \sqrt{2}A_n(T_1)e^{i\omega_n T_0} \sin(3m\pi x) + \text{C.C.} \tag{106}$$

Substituting w_0 from Eq. (106) into Eq. (12) yields

$$\begin{aligned} D_0^2 w_1 + w_1^{iv} + Pw_1'' + k_1 w_1 &= -2\sqrt{2}i[\omega_m A_m'(T_1)e^{i\omega_m T_0} \sin(m\pi x) \\ &+ \omega_n A_n'(T_1)e^{i\omega_n T_0} \sin(3m\pi x)] \\ &- 2\sqrt{2}k_3[A_m^3(T_1)e^{3i\omega_m T_0} \sin^3(m\pi x) \\ &+ A_n^3(T_1)e^{3i\omega_n T_0} \sin^3(3m\pi x) \\ &+ 3A_m^2(T_1)\bar{A}_m(T_1)e^{i\omega_m T_0} \sin^3(m\pi x) \\ &+ 3A_n^2(T_1)\bar{A}_n(T_1)e^{i\omega_n T_0} \sin^3(3m\pi x) \\ &+ 3A_n(T_1)A_m^2(T_1)e^{i(\omega_n+2\omega_m)T_0} \\ &\times \sin(3m\pi x) \sin^2(m\pi x) \\ &+ 3A_n(T_1)\bar{A}_m^2(T_1)e^{i(\omega_n-2\omega_m)T_0} \\ &\times \sin(3m\pi x) \sin^2(m\pi x) \\ &+ 3A_n^2(T_1)A_m(T_1)e^{i(2\omega_n+\omega_m)T_0} \\ &\times \sin^2(3m\pi x) \sin(m\pi x) \\ &+ 3A_n^2(T_1)\bar{A}_m(T_1)e^{i(2\omega_n-\omega_m)T_0} \\ &\times \sin^2(3m\pi x) \sin(m\pi x) \\ &+ 6A_n(T_1)A_m(T_1)\bar{A}_m(T_1)e^{i\omega_n T_0} \\ &\times \sin(3m\pi x) \sin^2(m\pi x) \\ &+ 6A_m(T_1)A_n(T_1)\bar{A}_n(T_1)e^{i\omega_m T_0} \\ &\times \sin(m\pi x) \sin^2(3m\pi x)] + \text{C.C.} + \dots \tag{107} \end{aligned}$$

Now, we consider the simply supported boundary condition:

$$w_1 = w_1'' = 0 \quad \text{at } x = 0 \text{ and } x = 1. \tag{108}$$

Based on the methodology given in [24], the solvability conditions of Eq. (107) will be

$$\begin{aligned} i\omega_m A_m'(T_1) &= -\frac{9}{4}k_3 A_m^2(T_1)\bar{A}_m(T_1) \\ &- 3k_3 A_m(T_1)A_n(T_1)\bar{A}_n(T_1) \\ &+ \frac{3}{4}k_3 A_n(T_1)\bar{A}_m^2(T_1)e^{i\sigma T_1} \tag{109} \end{aligned}$$

and

$$\begin{aligned} i\omega_n A_n'(T_1) &= -\frac{9}{4}k_3 A_n^2(T_1)\bar{A}_n(T_1) \\ &- 3k_3 A_m(T_1)\bar{A}_m(T_1)A_n(T_1) \\ &+ \frac{1}{4}k_3 A_m^3(T_1)e^{-i\sigma T_1} \tag{110} \end{aligned}$$

where in Eqs. (109) and (110) the amplitudes $A_m(T_1)$, $A_n(T_1)$ in polar form are defined by $A_m(T_1) = \frac{1}{2}a_m(T_1)e^{i\beta_m(T_1)}$, $A_n(T_1) = \frac{1}{2}a_n(T_1)e^{i\beta_n(T_1)}$. Moreover, the symbol σ known as internal detuning parameter is defined by

$$\sigma = \omega_n - 3\omega_m \quad \text{with } m = 1, 2, 3, \dots \text{ and } n = 3m. \tag{111}$$

Solution of Eq. (107) subject to the boundary conditions given in Eq. (108) will be

$$\begin{aligned} w_1(x, T_0, T_1) &= -\frac{\sqrt{2}}{2}k_3[f_1(x)A_m^3(T_1)e^{3i\omega_m T_0} \\ &+ f_2(x)A_n^3(T_1)e^{3i\omega_n T_0} \\ &+ f_3(x)A_m^2(T_1)\bar{A}_m(T_1)e^{i\omega_m T_0} \\ &+ f_4(x)A_n^2(T_1)\bar{A}_n(T_1)e^{i\omega_n T_0} \\ &+ f_5(x)A_n(T_1)A_m^2(T_1)e^{i(\omega_n+2\omega_m)T_0} \\ &+ f_6(x)A_n(T_1)\bar{A}_m^2(T_1)e^{i(\omega_n-2\omega_m)T_0} \\ &+ f_7(x)A_n^2(T_1)A_m(T_1)e^{i(2\omega_n+\omega_m)T_0} \\ &+ f_8(x)A_n^2(T_1)\bar{A}_m(T_1)e^{i(2\omega_n-\omega_m)T_0} \\ &+ f_9(x)A_n(T_1)A_m(T_1)\bar{A}_m(T_1)e^{i\omega_n T_0} \\ &+ f_{10}(x)A_m(T_1)A_n(T_1)\bar{A}_n(T_1)e^{i\omega_m T_0}] \\ &+ \text{C.C.} + \dots \tag{112} \end{aligned}$$

Substituting Eq. (112) into Eq. (107), using modulation Eqs. (109) and (110), equating the coefficients of the like harmonics of T_0 , noting that $n = 3m$ and replacing ω_n with $3\omega_m$, one gets

$$f_1^{iv}(x) + Pf_1''(x) + (k_1 - 9\omega_m^2)f_1(x) = 3 \sin(m\pi x), \tag{113}$$

$$f_2^{iv}(x) + Pf_2''(x) + (k_1 - 81\omega_m^2)f_2(x) = 3 \sin(3m\pi x) - \sin(9m\pi x), \tag{114}$$

$$f_3^{iv}(x) + Pf_3''(x) + (k_1 - \omega_m^2)f_3(x) = -3 \sin(3m\pi x), \tag{115}$$

$$f_4^{iv}(x) + Pf_4''(x) + (k_1 - 9\omega_m^2)f_4(x) = -3 \sin(9m\pi x), \tag{116}$$

$$f_5^{iv}(x) + Pf_5''(x) + (k_1 - 25\omega_m^2)f_5(x) = -3 \sin(m\pi x) + 6 \sin(3m\pi x) - 3 \sin(5m\pi x), \tag{117}$$

$$f_6^{iv}(x) + Pf_6''(x) + (k_1 - \omega_m^2)f_6(x) = 6 \sin(3m\pi x) - 3 \sin(5m\pi x), \tag{118}$$

$$f_7^{iv}(x) + Pf_7''(x) + (k_1 - 49\omega_m^2)f_7(x) = 6 \sin(m\pi x) + 3 \sin(5m\pi x) - 3 \sin(7m\pi x), \tag{119}$$

$$f_8^{iv}(x) + Pf_8''(x) + (k_1 - 25\omega_m^2)f_8(x) = 6 \sin(m\pi x) + 3 \sin(5m\pi x) - 3 \sin(7m\pi x), \tag{120}$$

$$f_9^{iv}(x) + Pf_9''(x) + (k_1 - 9\omega_m^2)f_9(x) = -6 \sin(m\pi x) - 6 \sin(5m\pi x), \tag{121}$$

$$f_{10}^{iv}(x) + Pf_{10}''(x) + (k_1 - \omega_m^2)f_{10}(x) = 6 \sin(5m\pi x) - 6 \sin(7m\pi x). \tag{122}$$

Moreover, substituting Eq. (112) into Eq. (108) and equating the coefficients of the like harmonics of T_0 yields

$$f_i(x) = f_i''(x) = 0 \quad \text{for } i = 1, 2, 3, \dots, 10$$

$$\text{at } x = 0 \text{ and } x = 1. \tag{123}$$

It should be noted that the functions f_1 to f_{10} can be analytically obtained out of the above ten uncoupled ODEs. However, for brevity, the detailed calculations are not included here. Having on hand the values of f_1

to f_{10} , the nonlinear normal mode $w(x, T_0, T_1)$ ($w = w_0 + \varepsilon w_1 + \dots$ with $\varepsilon = 1$) in the internal resonance condition that tends to the m th and $3m$ th linear modes can be expressed as

$$w(x, T_0, T_1) = \sqrt{2}A_m(T_1)e^{i\omega_m T_0} \sin(m\pi x) + \sqrt{2}A_n(T_1)e^{i\omega_n T_0} \sin(3m\pi x) - \frac{\sqrt{2}k_3}{2} \left[f_1(x)A_m^3(T_1)e^{3i\omega_m T_0} + f_2(x)A_n^3(T_1)e^{3i\omega_n T_0} + f_3(x)A_m^2(T_1)\bar{A}_m(T_1)e^{i\omega_m T_0} + f_4(x)A_n^2(T_1)\bar{A}_n(T_1)e^{i\omega_n T_0} + f_5(x)A_n(T_1)A_m^2(T_1)e^{i(\omega_n+2\omega_m)T_0} + f_6(x)A_n(T_1)\bar{A}_m^2(T_1)e^{i(\omega_n-2\omega_m)T_0} + f_7(x)A_n^2(T_1)A_m(T_1)e^{i(2\omega_n+\omega_m)T_0} + f_8(x)A_n^2(T_1)\bar{A}_m(T_1)e^{i(2\omega_n-\omega_m)T_0} + f_9(x)A_n(T_1)A_m(T_1)\bar{A}_m(T_1)e^{i\omega_n T_0} + f_{10}(x)A_m(T_1)A_n(T_1)\bar{A}_n(T_1)e^{i\omega_m T_0} \right] + \text{C.C.} + \dots \tag{124}$$

4.2 Steady-state stability analysis

To study the steady-state stability of the solutions in Eqs. (109) and (110) the method of eigenvalues-eigenvectors has to be employed. To do this, we take the amplitudes $A_m(T_1) = \frac{1}{2}a_m(T_1)e^{i\beta_m(T_1)}$, $A_n(T_1) = \frac{1}{2}a_n(T_1)e^{i\beta_n(T_1)}$ and insert them into Eqs. (109) and (110). Then, by separating real and imaginary parts in the obtained relations, one yields the following differential algebraic equations (DAEs):

$$a'_m = \frac{3}{16}k_3a_n a_m^2 \sin \gamma = g_1(a_m, a_n, \gamma), \tag{125}$$

$$a'_n = -\frac{1}{2\omega_n}k_3a_m^3 \sin \gamma = g_2(a_m, a_n, \gamma), \tag{126}$$

$$\gamma' = -2k_3 \left(-\frac{9}{32} \frac{a_n^2}{\omega_n} - \frac{3}{8} \frac{a_m^2}{\omega_n} + \frac{1}{4} \frac{a_m^3}{\omega_n a_n} \cos \gamma + \frac{27}{32} \frac{a_m^2}{\omega_m} + \frac{9}{8} \frac{a_n^2}{\omega_m} - \frac{9}{32} \frac{a_m a_n}{\omega_m} \cos \gamma \right) + \sigma = g_3(a_m, a_n, \gamma), \tag{127}$$

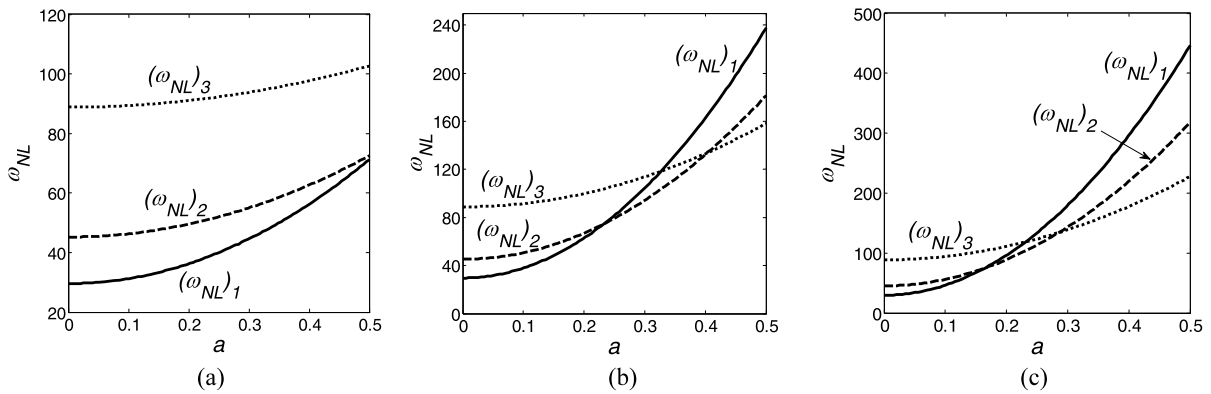


Fig. 2 Variation of dimensionless frequencies ω_{NL} ($(\omega_{NL})_1$, $(\omega_{NL})_2$ and $(\omega_{NL})_3$) vs. modal amplitude of vibration a with $k_1 = 9\pi^4$ and $P = \pi^2$; **(a)** $k_3 = 90\pi^4$, **(b)** $k_3 = 450\pi^4$, **(c)** $k_3 = 900\pi^4$

where

$$\gamma = \beta_n - 3\beta_m + \sigma T_1 \quad \text{where } n = 3m, \tag{128}$$

in which

$$\beta'_m = \frac{2k_3}{\omega_m a_m} \left(\frac{9}{32} a_m^3 + \frac{3}{8} a_m a_n^2 - \frac{3}{32} a_m^2 a_n \cos \gamma \right), \tag{129}$$

$$\beta'_n = \frac{2k_3}{\omega_n a_n} \left(\frac{9}{32} a_n^3 + \frac{3}{8} a_m^2 a_n - \frac{1}{4} a_m^3 \cos \gamma \right), \tag{130}$$

where g_1 , g_2 and g_3 are functions of a_m , a_n and γ . Again, it is emphasized that the prime over any parameter denotes the first derivative with respect to T_1 . For the steady-state response, we set $a'_m = a'_n = \gamma' = 0$. To check the stability condition of the steady-state solution, we linearize Eqs. (125)–(127) near singular (or steady-state) points. This will lead to a set of linear equations having constant coefficients multiplied by unknown disturbance terms. In other words, this is a typical case known as eigenvalue problem in the form $\{\mathbf{X}'\} = [\mathbf{A}]\{\mathbf{X}\}$ in which $\mathbf{X} = [a_m, a_n, \gamma]^T$ and $A_{ij} = \frac{\partial g_i(a_m, a_n, \gamma)}{\partial X_j}$ with $i, j = 1, 2$ and 3 , and A_{ij} is known as the *Jacobian matrix*. In the next step, $\det([\mathbf{A}] - \lambda[\mathbf{I}]) = 0$ is solved, out of which the eigenvalues (λ_i) of complex nature can be obtained. Now, the stability near singular points can be checked using these eigenvalues.

5 Results and case studies

5.1 Dynamic analysis in the non-internal resonance condition

Based on extracted equation (27) in conjunction with Eq. (28), a computer program has been written using MATLAB software out of which dimensionless linear and nonlinear results for the frequency and beam’s deflection, beam’s midspan time history can be calculated.

Figure 2 illustrates the first outcome of our computer program in which the variation of dimensionless beam nonlinear frequencies, i.e., $(\omega_{NL})_1$, $(\omega_{NL})_2$ and $(\omega_{NL})_3$, are plotted against dimensionless modal amplitude of vibration, a , in which $k_1 = 9\pi^4$, $P = \pi^2$ and the k_3/k_1 ratio is selected to be 10, 50 and 100. It can be seen from the figure that by increasing the value of k_3 , the value of nonlinear frequency increases accordingly. Moreover, the rate of variation of $(\omega_{NL})_1$ is greater than the other two frequencies. Referring to Eq. (28), if $k_3 = 0$, one deals with a linear problem in which it is clear that $(\omega_L)_{i+1} > (\omega_L)_i$ ($i = 1, 2, 3, \dots$). However, this not always can be true for a nonlinear problem ($k_3 \neq 0$) in which some modal amplitude range for example $(\omega_{NL})_1$ is greater than $(\omega_{NL})_2$ and $(\omega_{NL})_3$ (see Figs. 2b and c).

In the next step of our approximate-analytical solution, we try to obtain results for the beam’s deflection and time history of beam’s midspan. To do this, we primarily consider a general form for the beam’s deflection at $t = 0$ such as $w(x, 0) = H(x)$ yet to be obtained. In other words, $H(x)$ represents the amplitude of the beam deflection at $t = 0$. In order to comply

with the solution technique, instead of using $H(x)$ directly we prefer to employ the *Fourier Transform Series* of such a function in our solution methodology. Hence, after some mathematical simplifications on the *Fourier Transform Series* of Eq. (27) with $t = 0$, one gets the following general form:

$$\begin{aligned}
 h_i(x) &= \int_0^2 H(x) \sin(i\pi x) dx \\
 &= \sqrt{2}a_i + \frac{3\sqrt{2}k_3}{64\omega_i^2} a_i^3 + \frac{\sqrt{2}k_3}{64} \left[\frac{1}{9k^4\pi^4 - k_1} \right. \\
 &\quad \left. + \frac{3}{10k^4\pi^4 - k^2\pi^2 P} \right] a_k^3 \Big|_{i=3k}
 \end{aligned}$$

with $i = 1, 2, 3, \dots$. For example, in the case of a beam resting on a linear elastic foundation ($k_3 = 0$) for the first three modes of vibration one gets: $a_1|_{k_3=0,t=0} = h_1/\sqrt{2}$, $a_2|_{k_3=0,t=0} = h_2/\sqrt{2}$ and $a_3|_{k_3=0,t=0} = h_3/\sqrt{2}$, whereas in the case of a beam on a nonlinear foundation ($k_3 \neq 0$), a_i ($i = 1, 2, 3$) can be obtained by solving the following nonlinear coupled algebraic equations:

$$\left\{ \begin{aligned}
 \sqrt{2}a_1|_{k_3 \neq 0,t=0} + \frac{3\sqrt{2}k_3}{64\omega_1^2} a_1^3 \Big|_{k_3 \neq 0,t=0} &= h_1, \\
 \sqrt{2}a_2|_{k_3 \neq 0,t=0} + \frac{3\sqrt{2}k_3}{64\omega_2^2} a_2^3 \Big|_{k_3 \neq 0,t=0} &= h_2, \\
 \sqrt{2}a_3|_{k_3 \neq 0,t=0} + \frac{3\sqrt{2}k_3}{64\omega_3^2} a_3^3 \Big|_{k_3 \neq 0,t=0} \\
 = h_3 - \frac{\sqrt{2}k_3}{64} \left[\frac{1}{9\pi^4 - k_1} \right. \\
 \left. + \frac{3}{10\pi^4 - \pi^2 P} \right] a_1^3 \Big|_{k_3 \neq 0,t=0}
 \end{aligned} \right.$$

out of which a_i ($i = 1, 2, 3$) are derived in terms of h_i as an arbitrary inputs. Moreover, when one wants to compare the mode shapes, it is customary to normalize all the higher modes with respect to the mode number one. Now, with no restriction on the generality of the solution method, we assume some arbitrary values for h_i , such as $h_2/h_1 = 0.1$ and $h_3/h_1 = 0.001$ and $h_i/h_1|_{i>3} = 0$. Under these conditions the a_i are calculated. Therefore the dynamic response of the beam at $t = 0$ will be on hand to get through solution for $t > 0$. Figure 3 shows the deflection of

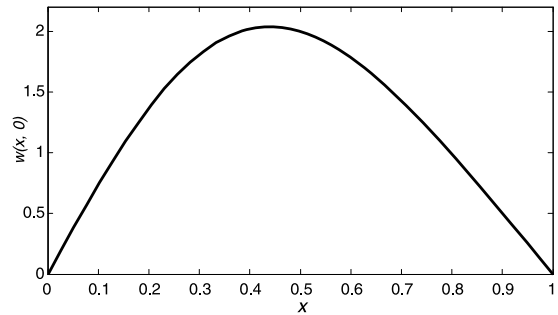


Fig. 3 Variation of deflection vs. x at an instant $t = 0$ for the known values of h_i , arbitrary values of k_3 , while $k_1 = 0.18\pi^4$ and $P = \pi^2$ using nine modes of vibration

the beam $w(x, t)$ at an instant $t = 0$ for the above-mentioned values of h_i , with arbitrary values of k_3 while $k_1 = 0.18\pi^4$ and $P = \pi^2$. Note that this result for the beam’s deflection is obtained by summation of the nine first modes of vibration.

Using first nine modes of vibration, Fig. 4 shows the general shape of deflection of the beam over entire length of the beam at an instant $t = 0.25$ for different values of $k_3 = 0, 10, 25, 50, 100$ and 250 , while $k_1 = 0.18\pi^4$ and $P = \pi^2$. The figure illustrates that when introducing an additional nonlinearity into the system, the absolute value of transverse dynamic deflection of the beam becomes smaller than those obtained for a linear elastic foundation, i.e., when $k_3 = 0$. Furthermore, it can be seen that by increasing the value of k_3 (nonlinear stiffness part) of elastic foundation, the peak value of deflection curve generally decreases. This means that an increase in the value of k_3 will cause an increase in the system stiffness.

Figure 5a shows the time history for deflection of a point at the middle of the beam resting on a nonlinear foundation $w(0.5, t)$ vs. time t ($0 < t < 0.5$) for different values of $k_3 = 0, 10, 25, 50, 100$ and 250 while $k_1 = 0.18\pi^4$ and $P = \pi^2$, using mode summation of the first nine modes. From Fig. 5a it can be seen that by increasing the value of nonlinear stiffness of the elastic foundation the maximum dynamic deflection of the beam remains almost the same but at a different time corresponding to the specified k_3 . In addition, referring to Fig. 5b it can be said that an increase in the value of k_3 will induce a higher vibration frequency (or smaller period). It should be noted that the same trend for variation of the beam deflection holds for $t > 0.5$.

Figure 6 shows the general deflection shape of the beam using its first nine modes over its entire length at

Fig. 4 Variation of deflection along length of the beam at $t = 0.25$ ($w(x, t = 0.25)$) for different values of $k_3 = 0, 10, 25, 50, 100$ and 250 , with $k_1 = 0.18\pi^4$ and $P = \pi^2$

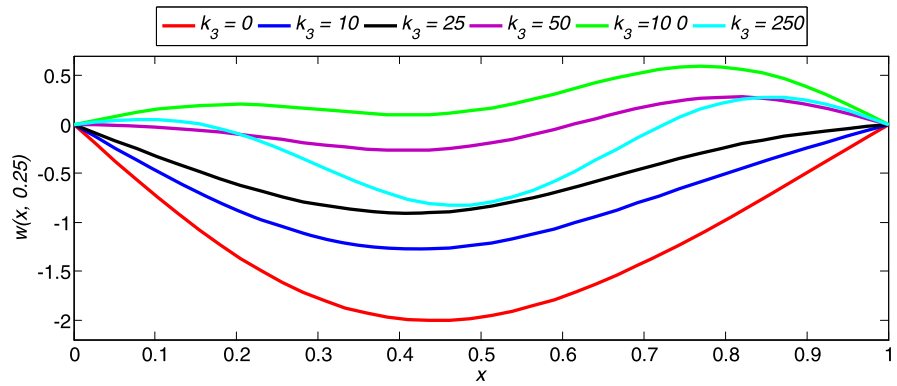
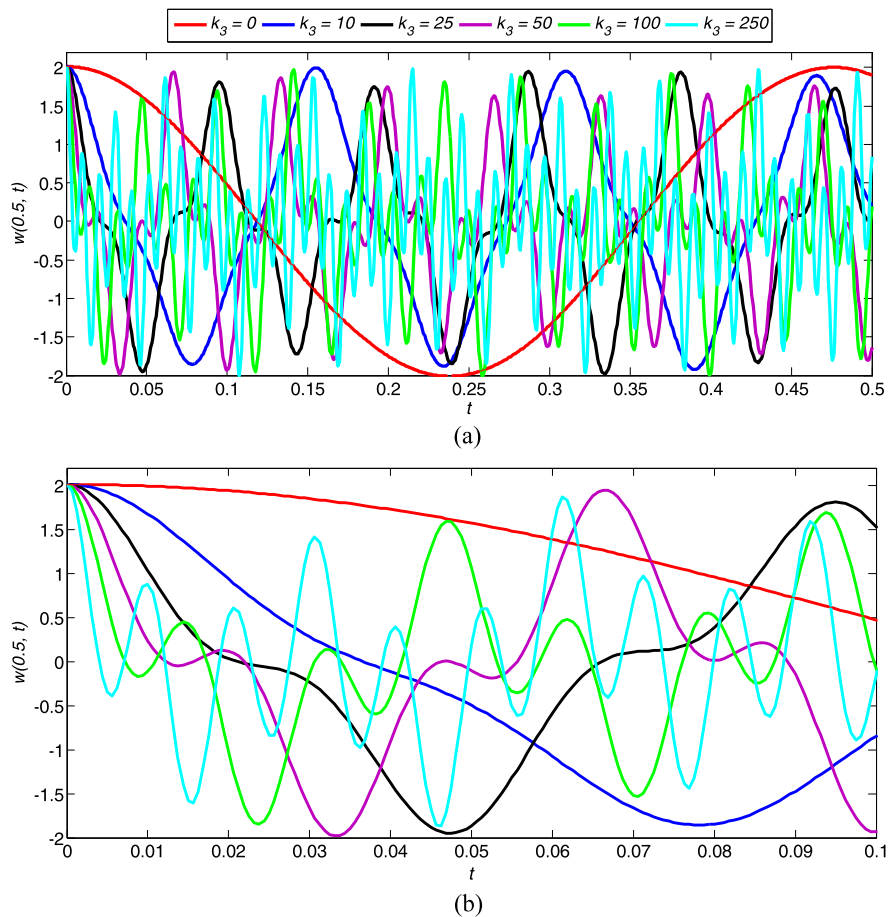


Fig. 5 Time history of the middle-point deflection of the beam $w(0.5, t)$ vs. time t for different values of $k_3 = 10, 25, 50, 100$ and 250 , while $k_1 = 0.18\pi^4$ and $P = \pi^2$; (a) Time history for interval $0 < t < 0.5$, (b) Part (a) magnified for time interval of $0 < t < 0.1$



an instant $t = 0.25$ with $P = \pi^2$, for different values of $k_1 = (0.18, 0.36, 0.54, 0.72)\pi^4$ while $k_3 = 0$ and $90\pi^4$. A close inspection of the figure reveals that for the case of linear foundation ($k_3 = 0$) by increasing the value of k_1 , somehow the trend of beam curvature changes its sign. Moreover, for the case of $k_3 = 90\pi^4$ the peak value of the deflection increases by increas-

ing the values of k_1 . However, it is worth to mention that this trend might change at other instants.

Figure 7 shows deflection of the central point of the beam resting on a foundation, i.e. $w(0.5, t)$ of first nine modes vs. time, with different values of $k_1 = (0.18, 0.36, 0.54, 0.72)\pi^4$ and $k_3 = 0$ and $90\pi^4$ while $P = \pi^2$. It can be seen that by increasing the

Fig. 6 Variation of deflection of the beam at $t = 0.25$ where $P = \pi^2$, for different values of k_1 and k_3 ; (-----) $k_3 = 0$ and (—) $k_3 = 90\pi^4$

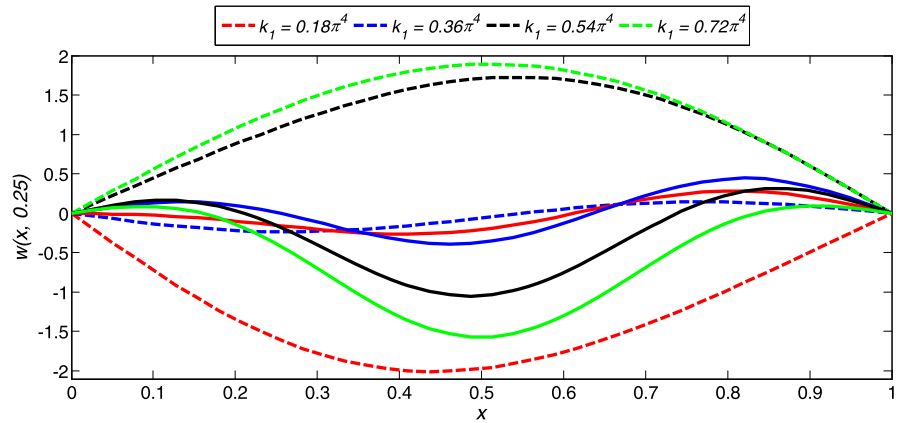


Fig. 7 Time history of deflection of the middle-point of the beam $w(0.5, t)$ vs. time t where $P = \pi^2$, for different values of k_1 and k_3 ; (-----) $k_3 = 0$ and (—) $k_3 = 90\pi^4$

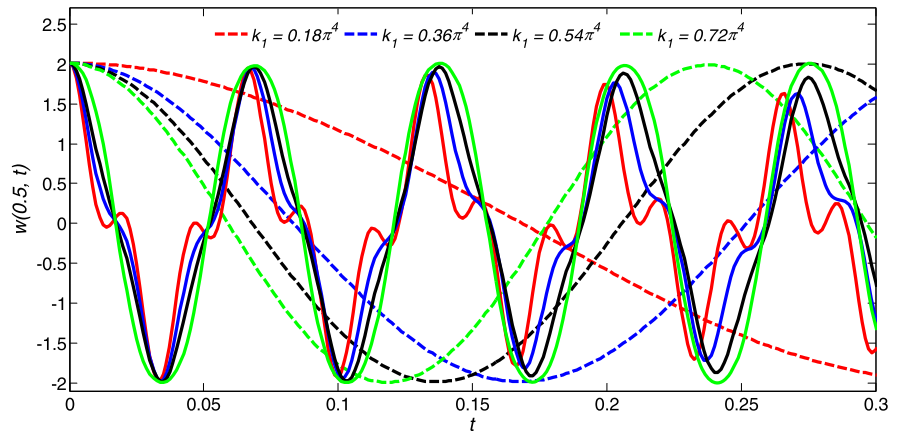
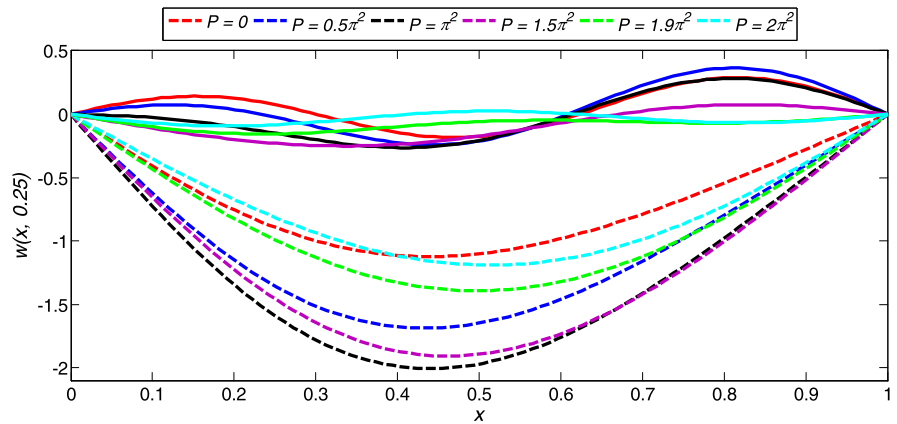


Fig. 8 Deflection of the beam resting on an elastic foundation using nine modes at $t = 0.25$ with $k_1 = 0.18\pi^4$, for different values of P and k_3 ; (-----) $k_3 = 0$ and (—) $k_3 = 90\pi^4$



value of linear stiffness of elastic foundation, i.e. k_1 , the vibration period decreases, as it could be expected.

Figure 8 shows the deflection of the beam resting on an elastic foundation using nine modes of vibration at $t = 0.25$ with $k_1 = 0.18\pi^4$, in which compressive

axial force and nonlinear stiffness values of foundation can vary such as $P = (0, 0.5, 1, 1.5, 1.9, 2)\pi^2$ and $k_3 = 0$ and $90\pi^4$, respectively. It can be observed that by increasing the value of k_3 the peak values of deflection curve decrease for the same values of compressive axial load P .

Fig. 9 Time history of deflection of the middle-point of the beam $w(0.5, t)$ vs. time t where $k_1 = 0.18\pi^4$, for different values of P and k_3 ; (-----) $k_3 = 0$ and (—) $k_3 = 90\pi^4$

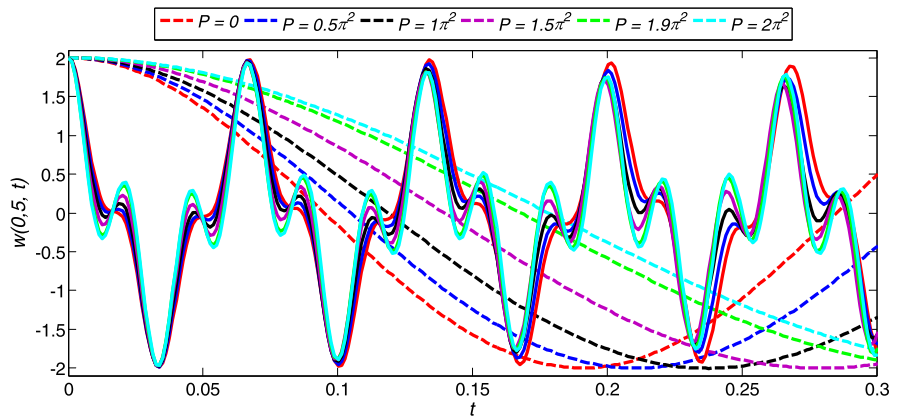


Figure 9 shows a midpoint deflection time history of the nine first modes of vibration of the beam resting on a linear foundation with $k_1 = 0.18\pi^4$ for different values of $P = (0, 0.5, 1, 1.5, 1.9, 2)\pi^2$ and $k_3 = 0$ and $90\pi^4$. It can be seen that by increasing the value of nonlinear stiffness of elastic foundation, i.e. k_3 , the peak values of deflection curve slightly decrease for the same values of compressive axial load P , where by increasing the value of nonlinear stiffness of elastic foundation, i.e. k_3 , the frequency of vibrations increases.

5.2 Results of dynamic and steady-state stability analyses in the case of 3:1 internal resonance

5.2.1 Dynamic response

Based on the dynamic response analysis in the case of 3:1 internal resonance mentioned in Sect. 4.1, a computer program is developed using MATLAB solver package, out of which different results can be obtained by changing different parameters.

Figure 10 shows the variation of k_1 vs. σ for different values of $P/P_{cr} = 0, 0.1, 0.2, 0.3, 0.4, 0.5, 0.6, 0.7, 0.8, 0.9$ and 1 ($P_{cr} = 10m^2\pi^2$ with $m = 1$) with $k_3 = 10$. It should be mentioned that σ has an upper limit which can be obtained from relation $\omega_m = 0$ for every value of P . This limiting condition for different values of P is shown by a dashed curve in Fig. 10. On the other hand, k_1 should always be physically greater than zero, which corresponds to $\sigma_{max} =$

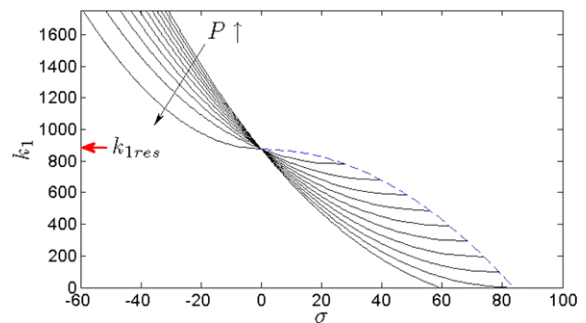


Fig. 10 Variation of k_1 vs. σ for different values of P with $k_3 = 10$ and $m = 1$

$\min(\sigma |_{\omega_m=0}, \sigma |_{k_1=0})$, where

$$\sigma |_{\omega_m=0} = \sqrt{8m^2\pi^2(10m^2\pi^2 - P)} \quad \text{and}$$

$$\sigma |_{k_1=0} = \sqrt{(3m\pi)^4 - P(3m\pi)^2} - \sqrt{(m\pi)^4 - P(m\pi)^2}.$$

Note that in this figure $k_{1res} = 876.7$, which can be obtained from relation $k_1 = 9m^4\pi^4$ with $m = 1$ in the case of 3:1 internal resonance.

Based on the aforementioned developed computer program and by incorporating outcome results extracted from Fig. 10, the midpoint deflection time history of the beam resting on a foundation in time interval $0 \leq t \leq t_1$, where $t_1 = 4\pi/\omega_{1res}$ ($\omega_{1res} = k_1 + \pi^4 + P\pi^2$), for different values of k_3 when $P = 0, \sigma = 0$ and $m = 1$, is shown in Fig. 11. From the figure it can be seen that by increasing the value of nonlinear stiffness of the elastic foundation, i.e. k_3 , the peak values of deflection curve slightly increase.

Fig. 11 Deflection of the middle-point of the beam $w(0.5, t)$ vs. time t for different values of $k_3 = 0, 100$ and 1000 with $P = 0, \sigma = 0$ and $m = 1$

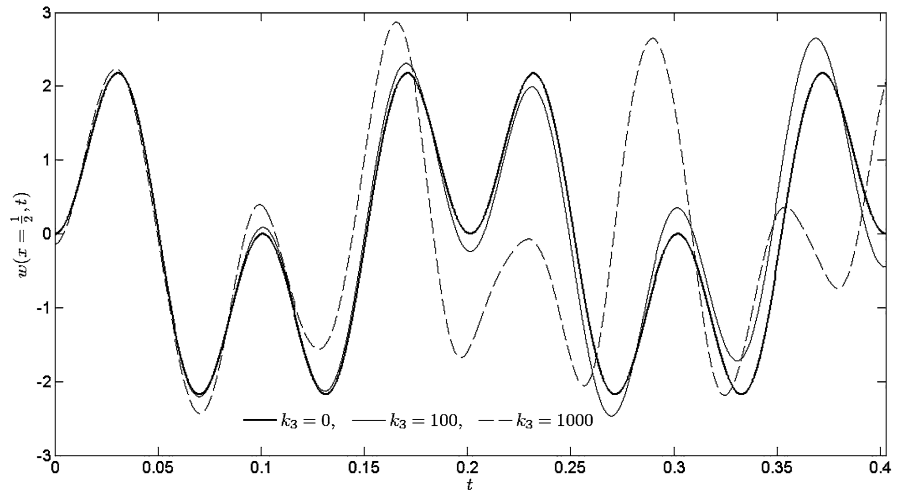


Fig. 12 Deflection of the middle-point of the beam $w(0.5, t)$ vs. time t for different values of $P/P_{cr} = 0, 0.1$ and 0.2 with $k_3 = 100, \sigma = 0, m = 1$

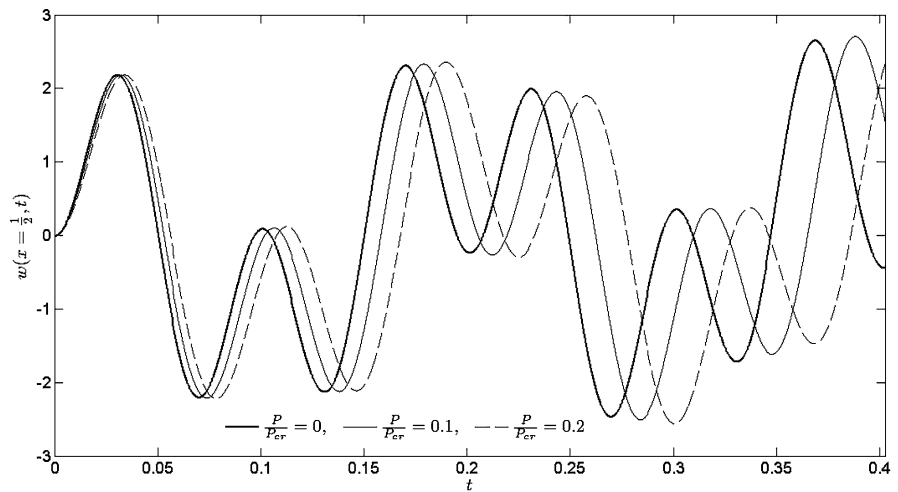


Figure 12 shows midpoint deflection time history of the beam resting on a foundation in time interval $0 \leq t \leq t_1$ for different values of P/P_{cr} with $k_3 = 100, \sigma = 0, m = 1$. From this figure it can be observed that by increasing the value of P/P_{cr} , the peak values of deflection curve shift a bit toward the right.

Figure 13 shows midpoint deflection of the beam resting on a nonlinear foundation in time interval $0 \leq t \leq t_1$ for different values of σ with $P = 0, k_3 = 10$ and $m = 1$. From the figure one can see that the effect of detuning parameter σ on the dynamic response is quite significant.

Figure 14 shows the general deflection shape of the beam at a time $t = 4\pi/\omega_{1res}$ ($w(x, t = 4\pi/\omega_{1res})$) for different values of k_3 while $\sigma = 0, P = 0$ and $m = 1$.

Figure 15 shows the deflection of the beam resting on a foundation with variable compressive axial force

at an instant $t = 4\pi/\omega_{1res}$ with $\sigma = 0, k_3 = 100$ and $m = 1$.

Figure 16 shows the deflection of the beam resting on an elastic foundation at an instant $t = 4\pi/\omega_{1res}$ for different values of σ with $P = 0, k_3 = 10$ and $m = 1$. It can be seen that by increasing the absolute value of detuning parameter σ the peak values of the deflection curve increase where the negative values of σ correspond to the higher values for the deflection of similar positive σ .

5.2.2 Results of steady-state stability analysis

Based on the stability analysis for the steady-state responses conducted in Sect. 4.2 and by incorporating outcome results extracted from Fig. 10, a 3-D variation of $a_m - \sigma - a_n$ for different P/P_{cr} values with $k_3 = 10$

Fig. 13 Deflection of the middle-point of the beam $w(0.5, t)$ vs. time t for different values of $\sigma = -10, -5, 0, 5, 10$ with $P = 0, k_3 = 10$ and $m = 1$

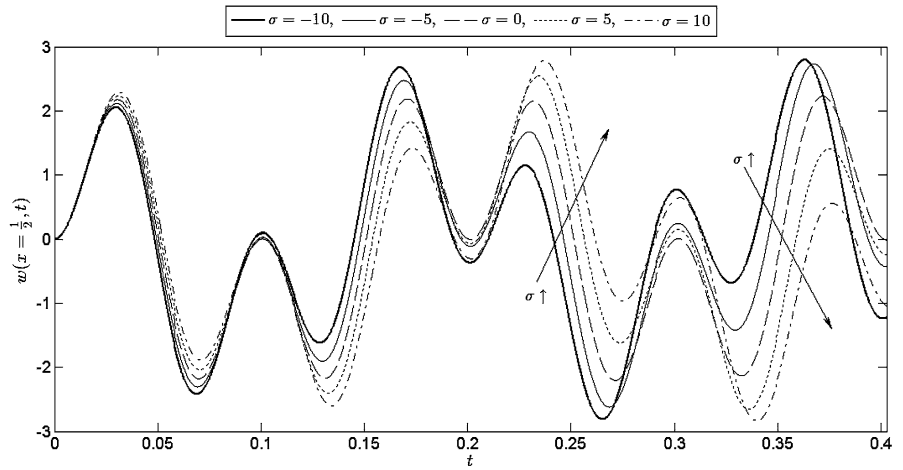


Fig. 14 Variation of deflection along length of the beam at an instant $t = 4\pi/\omega_{1res}$ for different values of $k_3 = 0, 100$ and 1000 with $\sigma = 0, P = 0$ and $m = 1$

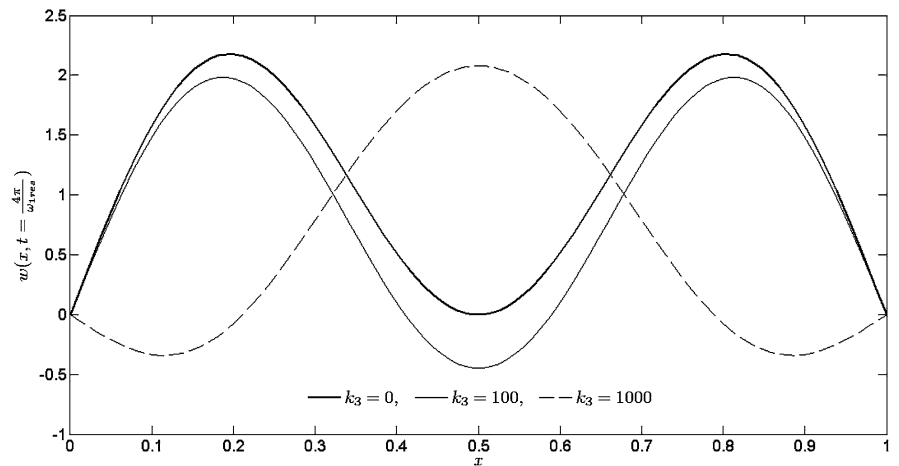


Fig. 15 Variation of deflection along length of the beam at an instant $t = 4\pi/\omega_{1res}$ for different values of $P/P_{cr} = 0, 0.1$ and 0.2 with $\sigma = 0, k_3 = 100$ and $m = 1$

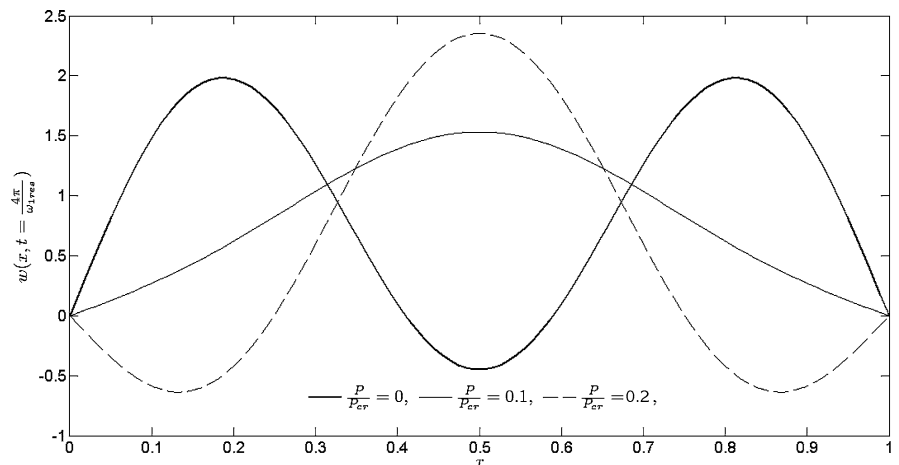


Fig. 16 Variation of deflection along the beam length at an instant $t = 4\pi/\omega_{1res}$ for different values of $\sigma = -10, -5, 0, 5$ and 10 with $P = 0, k_3 = 10$ and $m = 1$

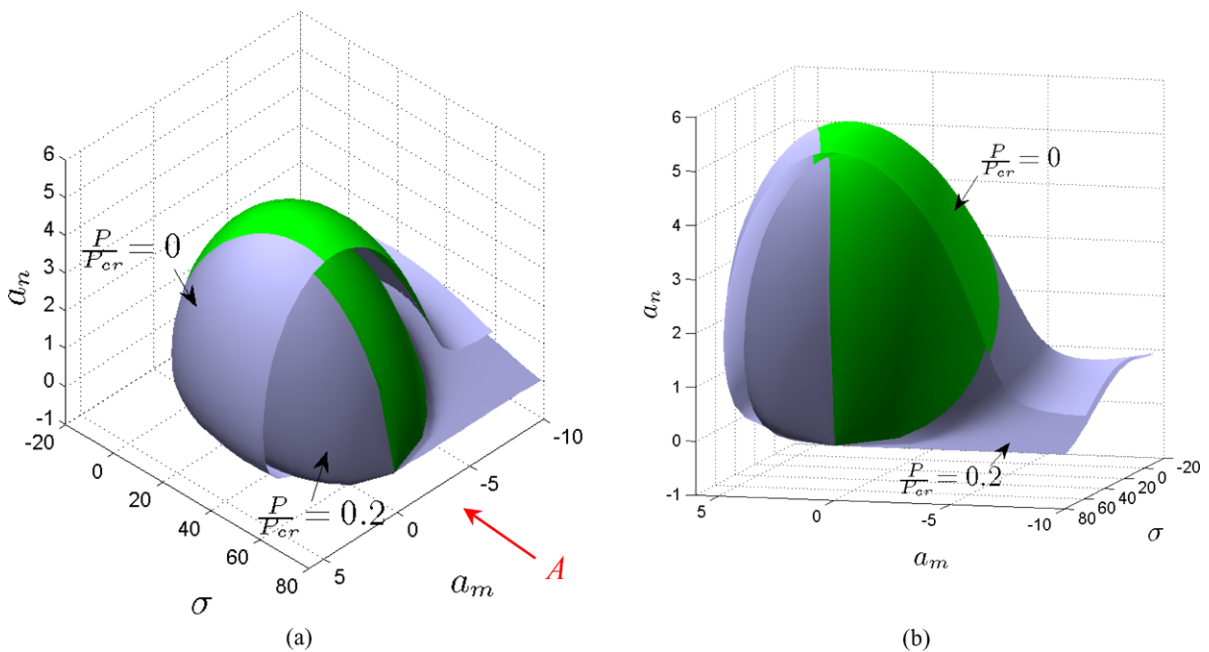
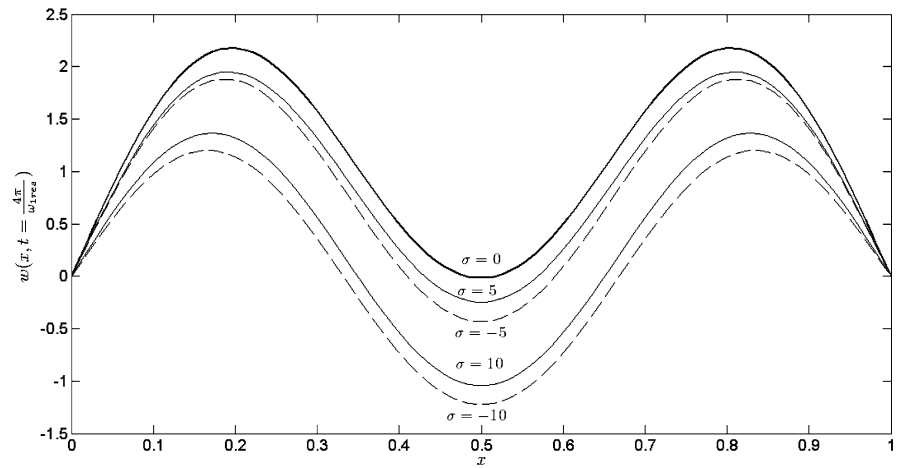


Fig. 17 Variations of the amplitudes a_n and a_m vs. detuning parameter σ for different compressive axial load $\frac{P}{P_{cr}} = 0$ and 0.2 with $k_3 = 10$ and $m = 1$. (a) The reference view; (b) View-A w.r.t. the reference view

and $m = 1$ is shown in Fig. 17. In this figure it should be noted that by increasing the value of compressive axial load P the 3-D surface will tend to shrink where for brevity only surfaces for two values of P/P_{cr} are shown. Moreover, it should be mentioned that these surfaces are plotted for $a_n > 0$ and for $a_n < 0$ similar surfaces exist. In addition, the green areas on these 3-D surface plots represent the unstable regions.

The three-dimensional surface plot of variation of amplitudes a_n and a_m vs. frequency detuning parameter

σ for $\frac{P}{P_{cr}} = 0.5, k_3 = 10$ and $m = 1$ is depicted in Fig 18. In this figure green regions represent the unstable regions.

Figure 19 is a two-dimensional representation of Fig. 18 in which the variation of nonlinear normal mode amplitude a_m is shown while detuning parameter σ is changing from -25 to 55 and the nonlinear normal mode amplitude a_n takes the values of $0.5, 1.16, 3$ and 5.6 . It should be noted that for the points with specific values of a_m, a_n and σ within the

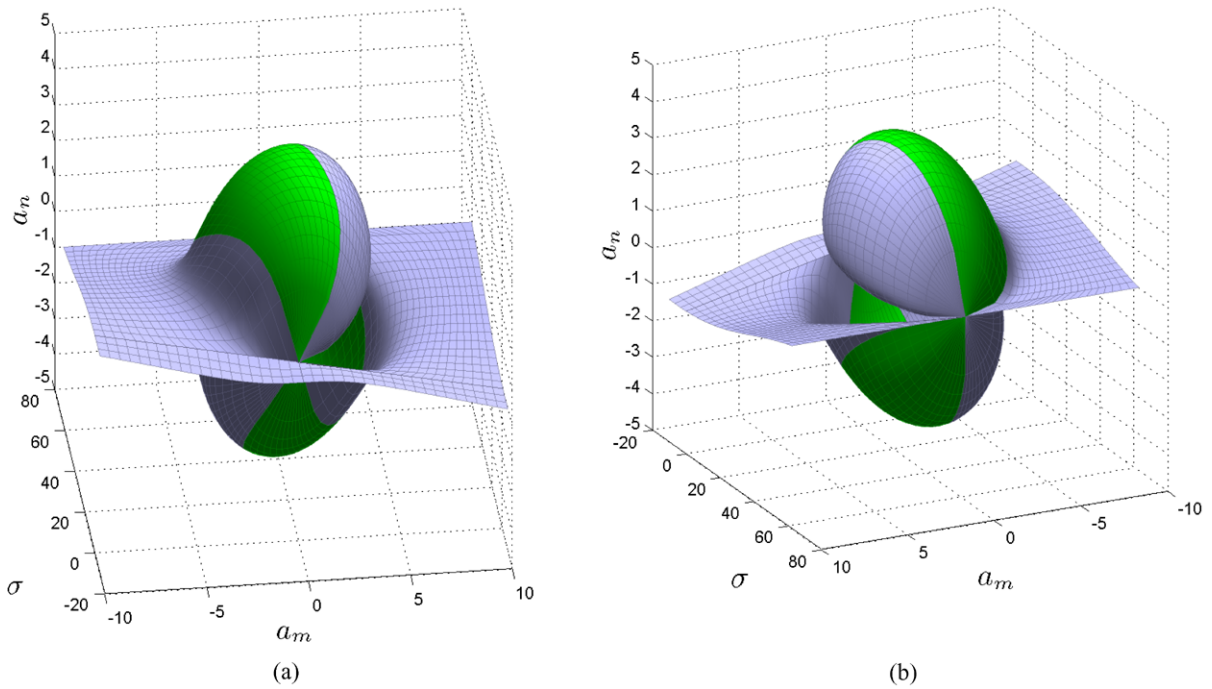


Fig. 18 Variations of the amplitudes a_n and a_m vs. detuning parameter σ with $\frac{P}{P_{cr}} = 0.5, k_3 = 10$ and $m = 1$. (a) The reference view; (b) 180° rotated view w.r.t. the reference view

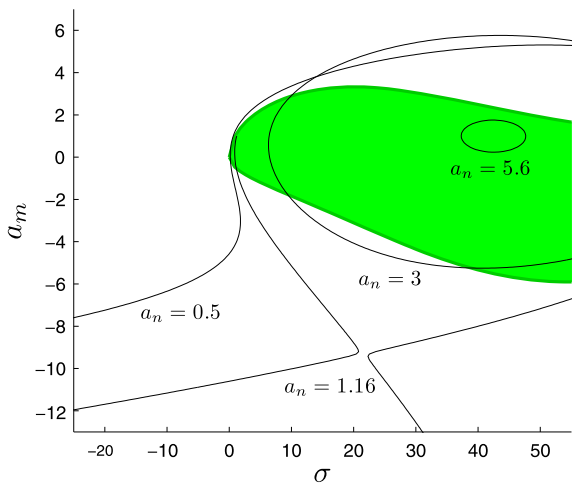


Fig. 19 Variation of amplitude a_m vs. frequency detuning parameter σ for $a_n = 0.5, 1.16, 3$ and $5.6, \frac{P}{P_{cr}} = 0.5, k_3 = 10$ and $m = 1$

green region the unstable condition is prevailing; for the points outside this region the system is in the stable condition.

Similarly to what has been done in Fig. 19, in the next step the variation of nonlinear normal mode am-

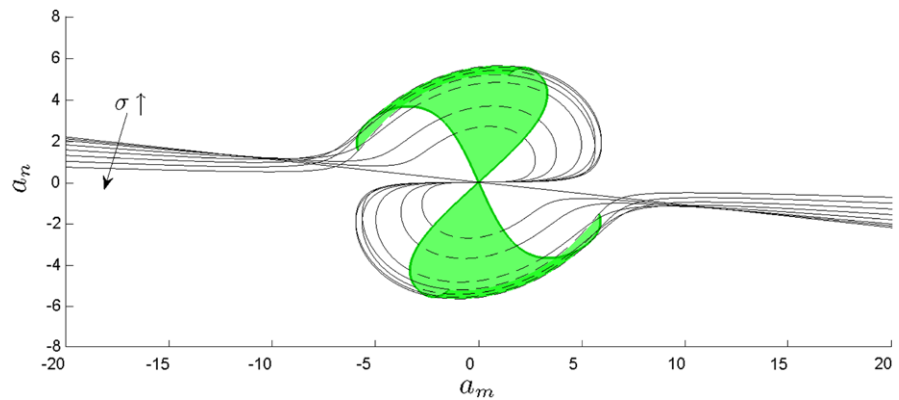
plitude a_n vs. nonlinear normal mode amplitude a_m for different values of $\sigma = 0, 5, 10, 20, 30, 40, 50$ and 60 with $k_3 = 10$ and $m = 1$ is illustrated in Fig. 20. Again, in this figure it should be noted that for the points with specific values of a_m, a_n and σ within the green region the unstable condition is prevailing; for the points outside this region the system is in the stable condition.

6 Conclusions

The nonlinear PDE governing dynamics of an Euler–Bernoulli beam resting on a nonlinear elastic foundation under axial compressive load is solved by using four different approximate-analytical nonlinear normal modes methods and the outcome results are as follows:

1. For the system under investigation it can be seen that there is the *three-to-one internal resonance* between the m th and $3m$ th modes and simultaneously the m th mode *critical compressive load* is seen accompanied with this internal resonance which is not seen when linear analysis is performed.

Fig. 20 Variation of nonlinear normal mode amplitude a_n vs. nonlinear normal mode amplitude a_m for $\sigma = 0, 5, 10, 20, 30, 40, 50$ and 60 with $\frac{P}{P_{cr}} = 0.5, k_3 = 10$ and $m = 1$



2. It can be seen that by increasing the values of k_3 , the values of nonlinear frequencies increase accordingly. Moreover, the trend of $(\omega_{NL})_1$ variation is greater than the other $(\omega_{NL})_{n|n>1}$.
3. In the no 3:1 internal resonant condition, when one introduces an additional nonlinearity into the system, for example k_3 , the absolute value of the dynamic deflection of the beam generally becomes smaller than those obtained if $k_3 = 0$.
4. Any increases in the value of k_3 will produce higher vibration frequency (or smaller period) for the case of no 3:1 internal resonant condition. In other words, as the nonlinearity k_3 increases, the contributions of $3m$ th mode become pronounced.
5. In the case of no 3:1 internal resonant condition and at the same level of compressive axial load P , it is observed that by increasing the value of k_3 the peak value of deflection curve slightly decreases.
6. In the 3:1 internal resonant condition it can be observed that by increasing the absolute value of detuning parameter, σ , the peak value of the deflection curves increases where the similar negative values of σ yield to the higher values of the deflection.
7. In the case of 3:1 internal resonance condition from NNMs steady-state analysis, the (σ, a_m, a_n) 3-D surface will tend to shrink in a nonlinear fashion as the value of compressive axial load P increases.

Open Access This article is distributed under the terms of the Creative Commons Attribution License which permits any use, distribution, and reproduction in any medium, provided the original author(s) and the source are credited.

References

1. Nayfeh, A.H., Lacarbonara, W., Chin, C.-M.: Nonlinear normal modes of buckled beams: three-to-one and one-to-one internal resonances. *Nonlinear Dyn.* **18**, 253–273 (1999)
2. Santee, D.M., Goncalves, P.B.: Oscillations of a beam on a non-linear elastic foundation under periodic loads. *Shock Vib.* **13**, 273–284 (2006)
3. Tsiatas, G.C.: Nonlinear analysis of non-uniform beams on nonlinear elastic foundation. *Acta Mech.* **209**, 141–152 (2010)
4. Kuo, Y.H., Lee, S.Y.: Deflection of nonuniform beams resting on a nonlinear elastic foundation. *Comput. Struct.* **51**, 513–519 (1994)
5. Hsu, M.H.: Mechanical analysis of non-uniform beams resting on nonlinear elastic foundation by the differential quadrature method. *Struct. Eng. Mech.* **22**, 279–292 (2006)
6. Oz, H.R., Pakdemirli, M., Ozkaya, E., Yilmaz, M.: Nonlinear vibrations of a slightly curved beam resting on a non-linear elastic foundation. *J. Sound Vib.* **212**, 295–309 (1998)
7. Pellicano, F., Mastroddi, F.: Nonlinear dynamics of a beam on elastic foundation. *Nonlinear Dyn.* **14**, 335–355 (1997)
8. Balkaya, M., Kaya, M.O., Saglam, A.: Analysis of the vibration of an elastic beam supported on elastic soil using the differential transform method. *Arch. Appl. Mech.* **79**, 135–146 (2009)
9. Birman, V.: On the effects of nonlinear elastic foundation on free vibration of beams. *J. Appl. Mech.* **53**, 471–474 (1986)
10. King, M.E., Vakakis, A.F.: An energy-based approach to computing resonant nonlinear normal modes. *J. Appl. Mech.* **63**, 810–819 (1996)
11. King, M.E., Vakakis, A.F.: An energy-based formulation for computing nonlinear normal modes in undamped continuous systems. *J. Vib. Acoust.* **116**, 332–340 (1994)
12. Vakakis, A.F.: Nonlinear mode localization in systems governed by partial differential equations. *Appl. Mech. Rev.* **49**, 87–99 (1996)
13. Pellicano, F., Vakakis, A.F.: Normal modes and boundary layers for a slender tensioned beam on a nonlinear foundation. *Nonlinear Dyn.* **25**, 79–93 (2001)

14. Jiang, D., Pierre, C., Shaw, S.W.: The construction of nonlinear normal modes for systems with internal resonance. *Int. J. Non-Linear Mech.* **40**, 729–746 (2005)
15. Pierre, C., Jiang, D., Shaw, S.W.: Nonlinear normal modes and their application in structural dynamics. *Math. Probl. Eng.* **2006**, Article ID 10847 (2006). 15 pp. doi:[10.1155/MPE/2006/10847](https://doi.org/10.1155/MPE/2006/10847)
16. Mazzilli, C.E.N., Sanches, C.T., Baracho, O.G.P., Wierciogroch, M., Keber, M.: Non-linear modal analysis for beams subjected to axial loads: analytical and finite-element solutions. *Int. J. Non-Linear Mech.* **43**(6), 551–561 (2008)
17. Casini, P., Giannini, O., Vestroni, F.: Persistent and ghost nonlinear normal modes in the forced response of non-smooth systems. *Physica D* (2011). doi:[10.1016/j.physd.2011.05.010](https://doi.org/10.1016/j.physd.2011.05.010)
18. Vestroni, F., Luongo, A., Paolone, A.: A perturbation method for evaluating nonlinear normal modes of a piecewise linear two-degrees-of-freedom system. *Nonlinear Dyn.* **54**, 379–393 (2008)
19. Casini, P., Vestroni, F.: Characterization of bifurcating nonlinear normal modes in piecewise linear mechanical systems. *Int. J. Non-Linear Mech.* **46**, 142–150 (2011)
20. Vakakis, A.F., Manevitch, L.I., Mikhlin, Y.V., Pilipchuk, V.N., Zevin, A.A.: *Normal Modes and Localization in Nonlinear Systems*. Kluwer Academic, Dordrecht (2001)
21. Vakakis, A.F., Gendelman, O.V., Bergman, L.A., McFarland, D.M., Kerschen, G., Lee, Y.S.: *Nonlinear Targeted Energy Transfer in Mechanical and Structural Systems*. Springer Science, Business Media, B.V., New York (2008)
22. Nayfeh, A.H.: *The Method of Normal Forms*. Wiley, New York (2011)
23. Murdock, J.A.: *Normal Forms and Unfoldings for Local Dynamical Systems*. Springer, New York (2003)
24. Nayfeh, A.H., Mook, D.T.: *Nonlinear Oscillations*. Wiley-Interscience, New York (1995)